8

Resistance of Flexible Emergent Vegetation and Their Effects on the Forces and Runup due to Waves

Sundar Vallam, Murali Kantharaj and Noarayanan Lakshmanan
Indian Institute of Technology Madras
India

1. Introduction

Field surveys of post great Indian Ocean tsunami of 2004 revealed that coastal vegetation can greatly improve the safety of coastal infrastructure. Buildings exposed to direct attack of the giant wave suffered greater damage than those fronted by vegetation. Thus, understanding the effect of vegetation on the hydrodynamic impact of such long waves on the coastal structures has become an important issue among the coastal engineering community. In the backdrop of such requirement, a comprehensive experimental program was taken up to investigate on the dynamic pressures exerted on a wall due to cnoidal waves in the presence and absence of a patch of elastic vertical cylinders. The patch of vertical cylinders is expected to replicate typical characteristics of vegetation of emerged type.

The resistance offered by vegetation to flow is essentially of drag in nature (Fischenich, 2000 and Darby, 1999) and is generally termed as, Green Belt effect. However, the nature of drag may be largely influenced by the hydro-elastic interaction of the current with the vegetal stems (Freeman, 1997). As such, stiffness of the vegetation appears to be one of the major parameters that govern the net drag offered to the flow. The percentage of reduction in the energy due to vegetation is also governed by the average diameter of the members within the vegetation, its height, distribution, density and type (Darby, 1999; Fischenich, 2000). In the past, several researchers have studied the flow characteristics past vegetal patches in open channels in order to evaluate friction factors for quantifying the resistance. However, measurements and quantification of resistance in the practical range of flow and vegetal parameters applicable to coastal protection are rather limited due to problems relating to scaling of all the fluid-structure physics.

1.1 Previous research

Frictional losses caused by momentum transfer through vegetated zone of a channel were the focus of most of the earlier investigations. Through a series of experiments using four species of coniferous trees in water and air, Fathi-Moghadam and Kouwen (1997) presented a model for estimating the drag coefficient of vegetation. Using this model, effects of flow depth and land slope on the *Darcy friction factor (f)* was investigated by Fathi-Moghadam (2006). Numerical and experimental works have been performed by Kutija *et al*. (2003) to

analyse and formulate the drag effects induced by vegetation. A vegetation index (E_{vi}) was proposed as one of the leading parameters to account for the effects of leaf density, shape and rigidity of individual trees. Meijer and Van Velzen (1999**),** Nepf (1999) and Dudley et al. (1998) reported the dependency of flow resistance on the density of the vegetation within the group and on the bending stiffness of the species. A formula for evaluation of vegetation resistance was proposed by Righetti and Armanini (2002) based on an analytical two layer model for sparsely distributed bushes under uniform flow conditions. The analytical model was verified with the experimental data.

The problem of vegetal resistance to flow can be categorised into submerged vegetation and emergent vegetation as claimed by (Liu et al., 2003). Since this study focuses on emergent vegetation, a concise review of relevant studies follows. Kouwen and Fathi-Moghadam (2000) and Jarvela (2004) investigated the variation in *f* due to vegetation in an open channel and concluded that the fundamental vegetation properties to be considered in establishing an equation for resistance are leaf density, shape, flexibility and manner of deflection of the tree species. Jarvela (2002) investigated the influence of the type, density and placement of vegetation, flow depth and velocity on friction losses. Large variations in the *f*, with depth of flow, velocity and vegetative density were observed. Further, the transition between submerged and partially submerged flow condition was observed to be at a depth of about 80% of the undeflected plant height.

Freeman *et al*. (2000), focussing mainly on *Manning's n,* argued that the equations, parameters, and methods developed by Ree and Crow (1977) and Kouwen and Li (1980) for a combined density and blockage of heavy ground cover and grasses do not produce satisfactory results. A methodology to determine flow resistance coefficients for submerged and partially submerged shrubs and woody vegetation was proposed. Data for developing the method were extracted from the study of Werth (1997), in which twenty natural plant species with both homogenous and mixed plant spacing were investigated with and without leaves. Unfortunately, a density measure such as leaf area was not recorded. Separate empirical regression equations were developed for the submerged and partially submerged cases revealing the modulus of elasticity to be a critical parameter, which can be estimated from the ratio of the un-deflected plant height to the stem diameter *H/d*, through field measurements. The approach of Freeman *et al*. (2000) does not directly take into consideration the deformation of foliage, as the stiffness modulus is a property of the stems. It appears not to be reasonable to assume that *E* can be related to only *H/d*, which implies that the differences in flexibility between species can be neglected. Later, Fathi-Moghadam (2006) proposed an empirical model to estimate the flow resistance coefficients (including the Darcy-Weisbach friction factor *f* and Manning's *n*) for flow inside emergent flexible vegetation.

The cantilever beam theory was used to compute the deflection of the flexible vegetation. In most of the earlier studies, the individual stems of the vegetation were simulated by a group of slender cylinders of constant height and diameter for the tandem configuration (Meijer and Van Velzen 1999). The results from experimental and numerical studies on the attenuation of incident wave energy by coastal forest including mangroves carried out by Hamzah *et al*. (1999) and Harada and Imamura (2006) are similar. The details of a pilot project on the integrated coastal vegetation in Sri Lanka are reported by Tanaka (2009). It is obvious that attention by researchers worldwide has been towards the understanding of the interaction of waves with vegetation.

A brief review of literature on the run-up due to long waves followed by pressures on vertical wall is discussed below. Hall and Watts (1953) proposed an empirical formula for run-up on an impermeable slope with an angle of 45^0 due to solitary waves. Carrier and Greenspan (1958) solved the shallow water equations analytically obtaining solutions for the prediction of the long wave run-up over smooth plane beaches. Synolakis (1986) investigated the run-up of non-breaking long waves theoretically by applying a power law to predict solitary wave run-up on a smooth plane beach. Other notable contributions on run-up of long waves over slopes are due to Li and Raichlen (2001), Carrier *et al*. (2003) and Hughes (2004).

An empirical formula of Goda (1974) to calculate pressures on vertical walls is widely adopted. Other salient contributions are due to Führböter (1993), and Müller and Whittaker (1993). It was generally concluded that sloping walls experience more load than vertical walls. Through experimental studies, Furukawa *et al*. (1997) demonstrated that the wave dissipation depends on forest density and the diameter of the tree trunks. The literature review thus indicates that information on wall pressures fronted by vegetation, in particular due to long waves, is scanty. This aspect in addition to the steady flow past vegetation is focussed through a well-controlled experimental program. Vegetative parameters, including the green belt width, stem diameter, spacing and their rigidity are varied resulting in a holistic view of the present wave vegetation interaction problem.

The effect of two prominent configurations of plantations, viz., tandem and staggered, in attenuating the wave induced pressures is studied. The vegetative parameters such as the width of the green belt (BG), diameter of the individual stems (D), their spacing (SP) were varied for an overall understanding of the steady floe or wave-vegetation interaction problem. Cnoidal waves were considered in the wave flume experiments in order to replicate the shallow water behaviour of tsunami as much as possible. The range of *Ursell parameter* considered for this purpose is 18 to 700.

2. Experimental program

2.1 Vegetation parameters

The mechanical characteristics of vegetation have a considerable effect on the resistance to flow of water. For tall vegetation, these properties include leaf density, shape and the general flexibility of tree species. To estimate the f due to flow through emerging and flexible vegetation, an index to account for the effects of the vegetation's mechanical characteristics is required. Since, the trees could be characterised similar to cantilever beams, the mechanical characteristics may be brought in through the resonance frequency of the first mode of vibration, namely the natural frequency of the vegetal stems. The natural frequency could be related to the '***Vegetation Index***' (Fathi-Moghadam 2007). The resonance frequencies are denoted as f_j (with $j = 1, 2, 3,..., n$, where f_1 is the fundamental or base natural frequency and $f_2,.., n$ are higher modes of natural frequencies). For a linear and homogeneous beam, f_j depends upon the beam's length l, mass per unit length m, second moment of inertia I, modulus of elasticity E, as well as a dimensionless parameter λj which in turn is a function of beam geometry and the boundary conditions under which it is tested. The mathematical relationship between the resonance frequency and the above variables may be written as (Timoshenko and Gere 1961),

$$f_j = \frac{\lambda_j^2}{2\pi}\left(\frac{EI}{ml^4}\right)^{0.5} \tag{1}$$

The above parameter characterizes the height, mass (including leaf density) and the moment of inertia of a tree. Herein, the beam length l is taken to be the height of the vegetal stem. According to Fathi-Moghadam (2007), on transferring the measurable parameters to the right side, the relationship between known and unknown group of variables involving the natural frequency of first mode, f_1, will be:

$$E_{vi} = f_1^2 \left(\frac{m_s}{l} \right) \tag{2}$$

where the total mass of the tree $m_s = ml$, and E_{vi} is called the **"vegetation index"** of a tree species. Measuring the height, mass and fundamental natural frequency of the tree, the vegetation index is estimated by the above equation.

2.2 Modelling of vegetation

Motivated by the need to study the hydro-elastic interaction of the flow with that of the vegetal stems, a suitable material for model tests had to be identified to represent coastal vegetation and mangroves in the real world. Yang and Choi (2009) indicated that the main effect of vegetal flexibility is the increase of Reynolds shear stresses and the intensity of turbulence in the vertical direction. Hence, reproducing the hydro-elastic behaviour is the key in understanding the effects of vegetation on pressures and run-up. One of the key parameter to study the hydro-elastic interaction of the flow with the vegetal stem to represent real-world coastal vegetation is Young's modulus E. Common timber has an E value in the range from 10.05 to 15GPa. Mangrove has maximum E values of 20.03GPa [Gan *et al*. (2001)].

To cover the wide range of E, a reference value of 14GPa was assumed for field condition, serving as a basis of the lab tests. In order to scale down the prototype values and identify the model material, assuming that the flow is due to storm surges and tsunamis, and considering also the experimental ranges of flow (including velocities and flow depth), a guiding scale ratio of 1:40, i.e., a Scale Factor (SF) of 40 was adopted. This would mean that the E value for the model material should be about 0.35Gpa, which is quite difficult to identify. The most practical option for achieving the above is to consider EI as a single parameter and scaling the rigidity. For the present study the material considered is Polyethylene with an E value of about 3.8 Gpa which is about ten times that of the required value. Since the rigidity is modelled herein, the above said variation could be compensated with the variation in I of the material. Having chosen the model material, the typical prototype dimensions of vegetal stems are considered in the range of 100mm – 400mm. Accordingly, using the Froude model law of scaling, the rigidity with the scale factor of $[SF]^5$ – the base diameter for model vegetation will fall in the range of 1.65 – 5.5 mm. The base diameter as arrived above only ensures that the bending action of the vegetal stems is properly scaled. Thus herein, the advantage of modelling rigidity rather than Young's modulus is clearly brought out. However, for accurate hydrodynamic interaction of the flow and stems, the hydrodynamic forces need to be correctly scaled as per Froude's Law. Considering Morison's force regime (Chakrabarti, 1983) the corresponding (to the above range) diameters for the exposed part of vegetal stems were arrived at In order to ensure that the change in diameter does not affect the bending behaviour of the model vegetation, a small clearance is provided between the base and the section, where the diameter changes from a lower to a higher value. It is to be mentioned that, the diameter at root is used only for calculation of EI of the vegetal stems.

2.3 Experimental parameters

The parameters that have been considered here include the size, elastic modulus of the vegetal stems, configuration of the vegetal patch or green belt, as well as the spacing between the individual plants within the green belt etc. Quantification of friction factor and energy loss in steady uniform flow is of primary interest and has practical relevance as far as long waves are concerned. For the measurement of pressures and forces on the structures mounted at a distance from the shoreline/reference line and run-up on mild slope of 1:30, a number of wave and beach parameters were considered in the wave flume experiments. The following variables are of interest for both currents and waves for investigating the response function such as resistance, force or run-up.

$$\text{Vegetal Response} = f(\rho, g, h, H, T, B_s, D, D_b, BG, f_1, l, SP, E, L, \beta, R_u, V), \tag{3}$$

where, ρ- mass density of water; g- gravitational acceleration; h- depth of water in the flume; H-wave height; T- Wave period; B_s- Width of the structure; D- diameter of the vegetation; D_b- diameter at the root of the vegetation; BG- width of green belt; f_1 –frequency of first mode of the vegetal stem; l- height of the vegetation; SP- centre to centre spacing between vegetation; E - modulus of plant stiffness; L- Wave length; β- Beach slope; R_u- Run-up; V– Flow velocity; The h refers to, h_s- depth of water at the toe of the structure; h_{avg}- average depth of water on the up-stream and down stream of flow in open channel.

The variables seen in equation (3) are grouped as per Buckingham's Pi theorem. The parameters thus obtained are tabulated in Table 1 in which, U_{max} is the velocity V and L_o is the deep water wave length. The non dimensional quantities investigated in the study are Darcy's f, and Manning's n in steady uniform flow and wave run-up R_u/H, pressures P^* and forces F^* on structures. They are designated as below.

$$f = \frac{8H_f gh}{LV^2} \tag{4}$$

$$F^* = \frac{F_{\max}}{0.5 * \rho g H^2 B_s} \tag{5}$$

$$P^* = \frac{P_{\max}}{H} \tag{6}$$

2.4 The test set-ups

Test facility for steady-uniform flow

The experiments were conducted in a horizontal, impermeable and rigid glass walled flume 10m long, 0.5m wide and 0.6m deep in the Hydraulics Laboratory at Indian Institute of Technology Madras, India. A head tank at one end served as a reservoir for the discharge into the flume, in which the water level could be maintained at a constant level by adjusting the inflow valve and the outflow weir. Closely spaced slender cylindrical members representing vegetation (with E=3.8E+09 N/m^2) were positioned at a distance of 6 m from one end of the flume in tandem configuration. On the down stream end, an over flow weir was used to adjust the desired flow depth. The water depth was recorded on the upstream

as well as on the downstream with a measuring scale fixed along the sides of the glass flume. The velocity on the upstream and downstream of the vegetation was measured with Bikini type propeller velocity meter.

The experiments were conducted for three different depths of flow (210 mm, 180 mm and 80 mm) for the tandem configuration considered herein. For each of above depths, three different widths of green belt of 250 mm, 625 mm and 1000 mm were employed for the tests. Two different diameter of vegetation of 10 mm and 3 mm for each of the green belt as mentioned earlier were adopted. Furthermore, for each of the two diameters considered, two different spacing (37.5 mm and 75 mm) were selected. Thus, for the present study, 12 different experimental set ups were considered. The schematic representation of the vegetation and flow parameters considered is shown in Fig.1 and typical configurations of vegetation for D = 10 mm, SP = 37.5 mm and 75 mm and BG = 1.0m, 0.625m and 0.250m is shown in Fig.2. The details of the flume and the experimental set-up for the tests with steady flow past vegetation are shown in Fig.3. The range of vegetation and flow parameters covered under the present study is provided in Table.1.

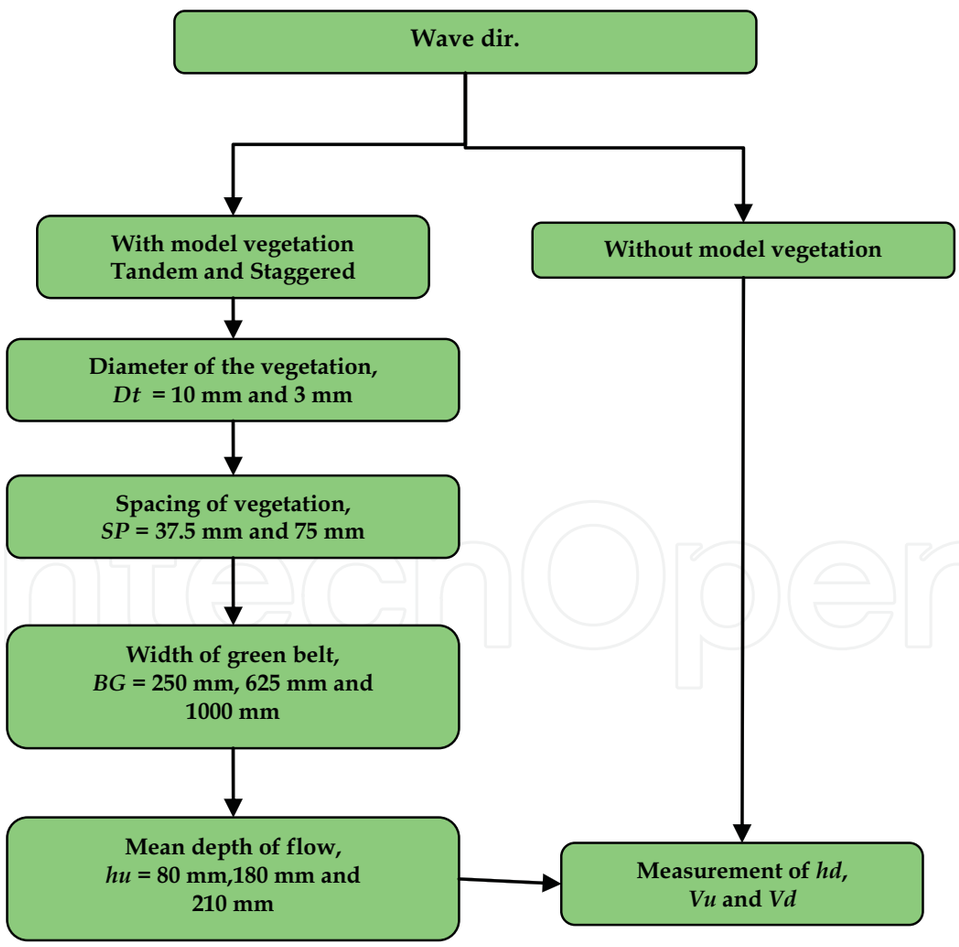

Fig. 1. Experimental Program for open channel flow experiments

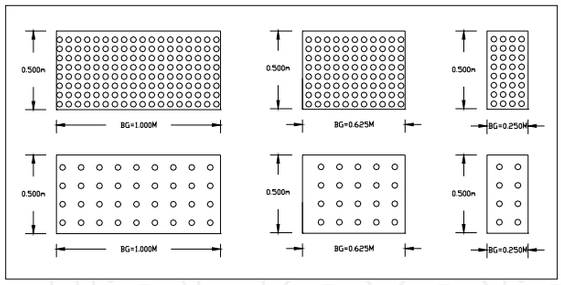

Tandem Configuration:
SP=0.0375 m and 0.075 m; D = 0.01 m.

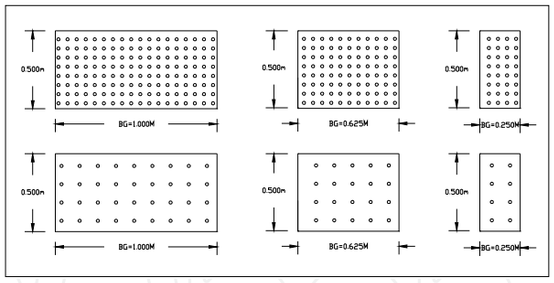

Tandem Configuration:
SP=0.0375 m and 0.075 m; D = 0.003 m.

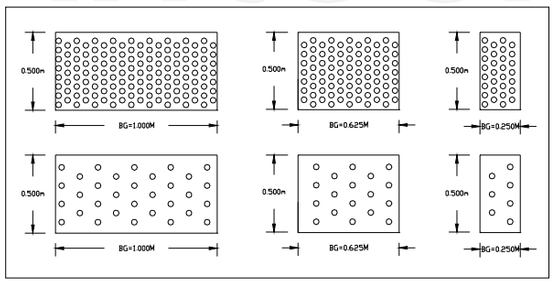

Staggered Configuration:
SP=0.0375 m and 0.075 m; D = 0.01 m.

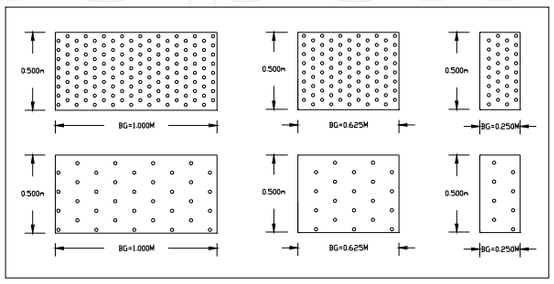

Staggered Configuration:
SP=0.0375 m and 0.075 m; D = 0.003 m.

Fig. 2. Different configurations of model stems used in open channel and wave flume tests.

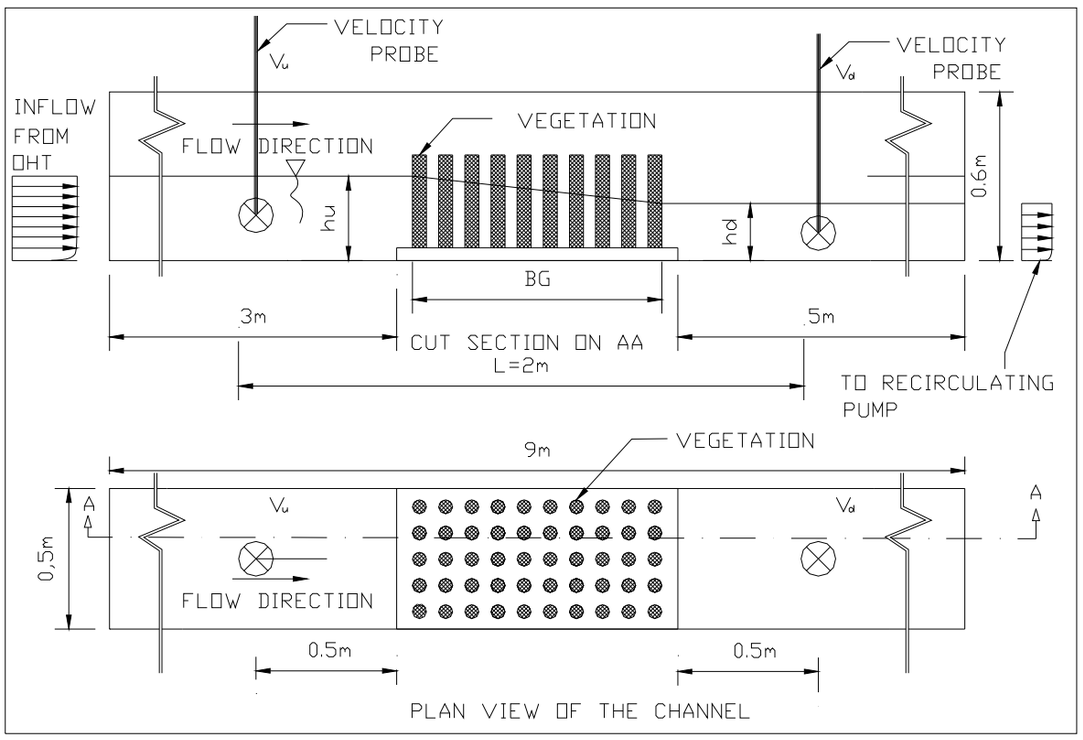

Fig. 3. Schematic diagram of test set-up in open channel for Tandem configuration.

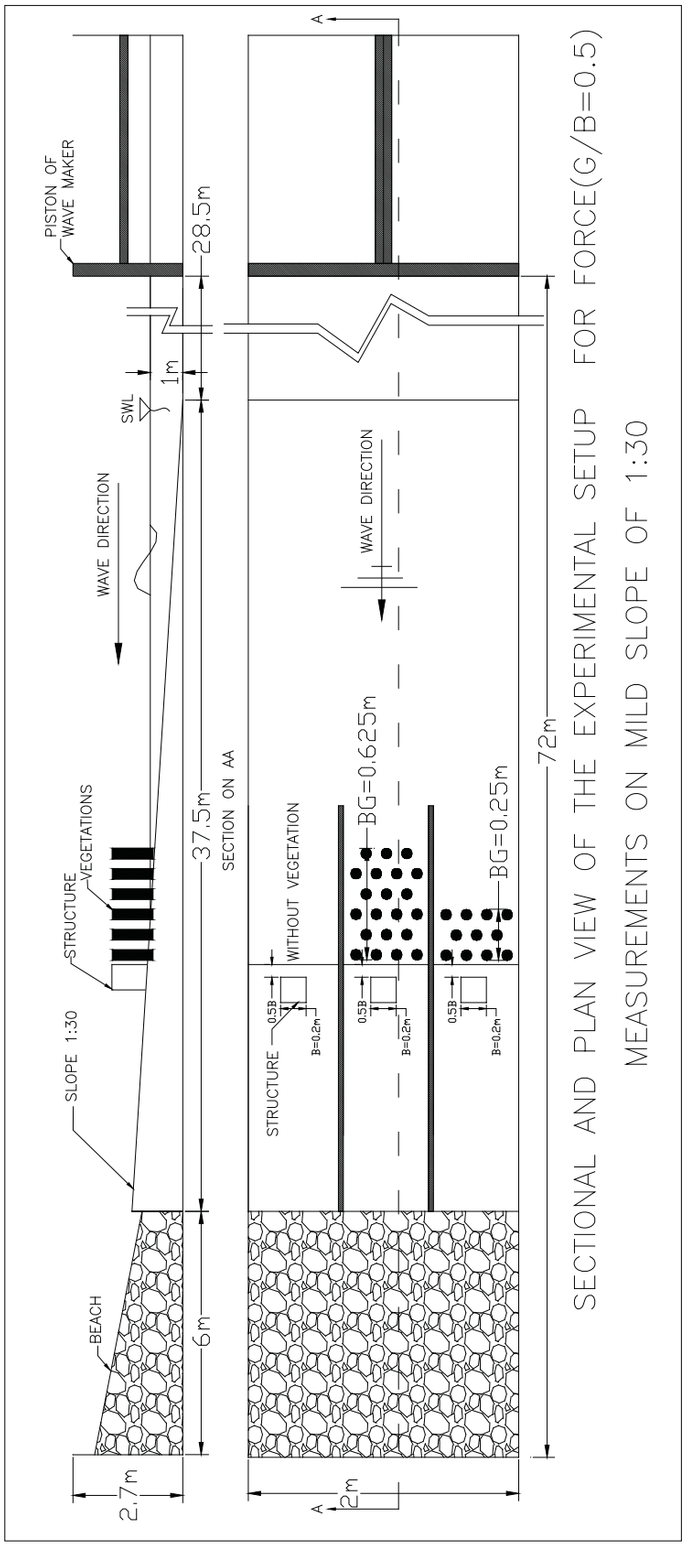

Fig. 4 (a). Experimental setup in the wave flume for measuring forces on model buildings fronted by vegetation.

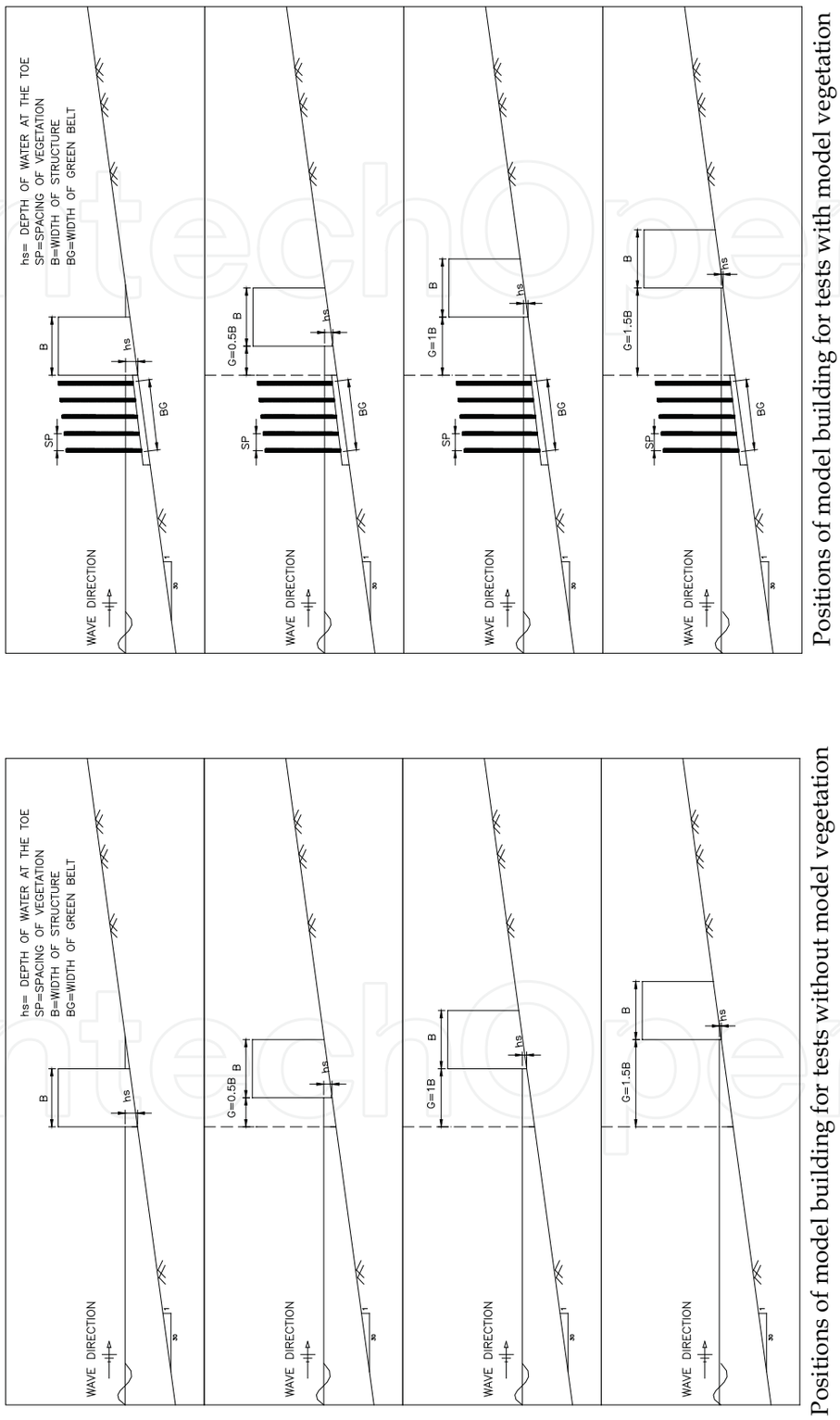

Fig. 4 (b). Conditions for which forces due to waves on a model building were measured.

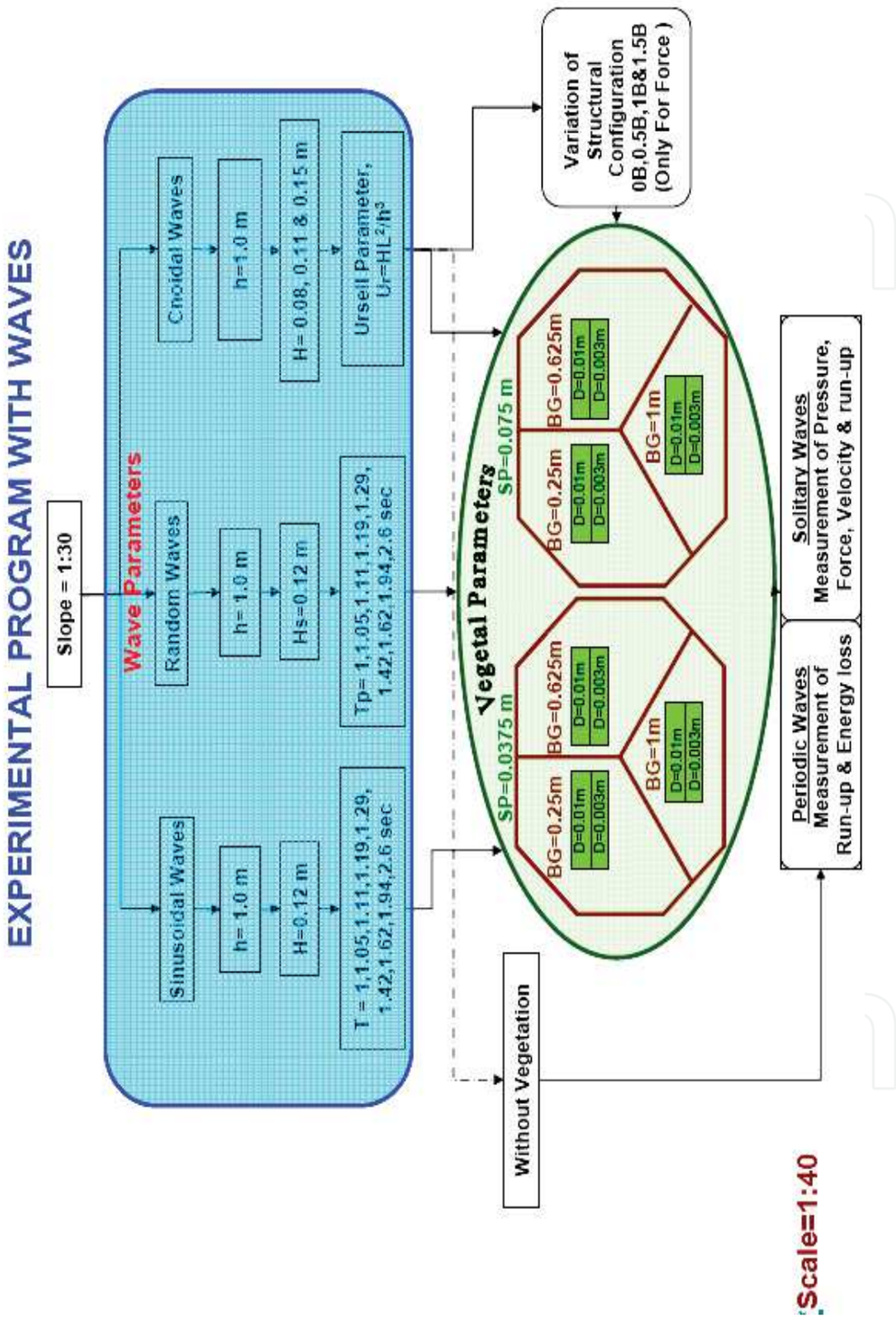

Fig. 4 (c). Experimental Programs for wave flume investigations for pressure, runup and force measurement.

BG=0.25 m and D = 0.003 m. *BG=0.25 m and D = 0.01 m.*

Fig. 5a. Typical views of flow gradient in the open channel tests (flow from left to right)

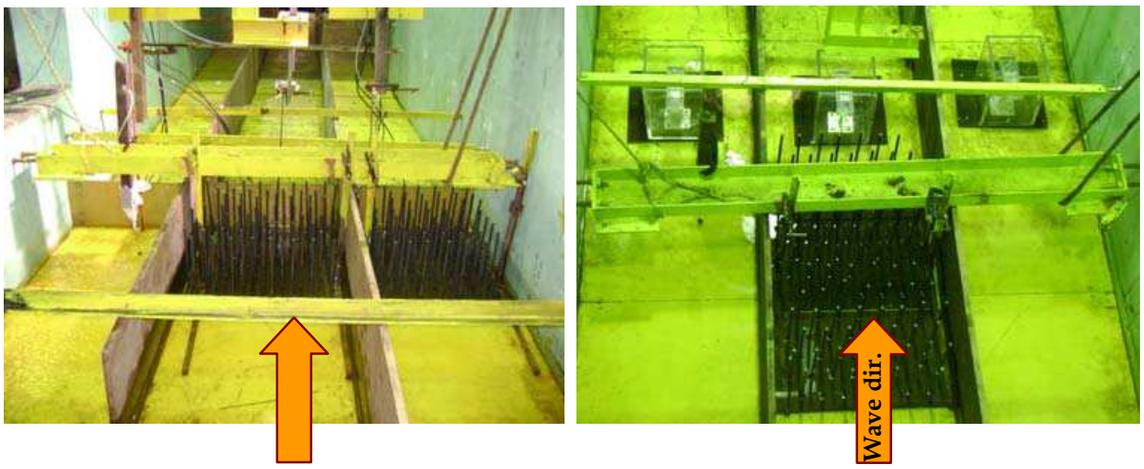

Fig. 5b. Typical views of model setup for run-up measurement (left) and force measurement (right). The model buildings could be seen with the instrumentation..

Froude Number , $F_r = \left(\frac{V_{avg}}{\sqrt{g * h}}\right)$	0.23 to 0.60
Relative spacing, $R_s = \left(\frac{SP}{D}\right)$	3.75,7.5,12.5 and 25
Velocity of ratio, $V_r = \left(\frac{V_{avg}}{f_1 D}\right)$	2.19 to 83
Frequency parameter, $f_z = \frac{1}{T}\left(\sqrt{\frac{h_{avg}}{g}}\right)$	0.247 to 1.42
Reynolds number, $\mathrm{Re} = \left(\frac{V_{avg} * h_{avg}}{\upsilon}\right)$	13693 to 146179
Vegetation-Flow Parameter, $VFP = \frac{EI(BG/D)}{\rho H l^3 V_{avg}^2 (SP/D)}$	0.001to 14.37
Vegetal parameter, $a = BG \cdot SP/D^2$	94 to 8333

Table 1. Range of dimensionless parameters covered in the present study

Among all the aforesaid parameters, the Vegetation-Flow Parameter, *VFP*, is newly introduced to obtain a unique parameter that combines the effects of structural rigidity of the individual model stem, flow and vegetation parameters. It is prudent to now recall the fact that, the earlier investigators have used the Vegetation Index as a parameter to classify vegetation (Fathi-Moghadam, 2007). However, it is to be mentioned that the Vegetation Index does not include parameters relating to rigidity *EI*, vegetation parameters *BG*, *SP/D* and the flow parameters. Hence, it is proposed that the present parameters derived from this work will be more relevant and comprehensive in view of the hydro-elastic processes being considered.

Flume facility for test in Waves

The present experimental study was carried out in a wave flume of 50 m long, 2.0 m wide and 2.7 m deep, in Department of Ocean Engineering, Indian Institute of Technology Madras, India. A computer controlled wave maker is installed at one end of the flume and on the other end; a rubble mound wave absorber is placed to minimize the reflection from the end of the flume. The water depth in the flume can be varied from 0.3 m to 2.0 m. For the present study, the water depth was maintained as 1.0 m and hence, the wave maker was operated in the piston mode. The wave generating system is capable of generating Sinusoidal, random waves, cnoidal and solitary waves. The wave maker can be operated either in piston mode or, in hinged mode primarily for the generation of deep-water waves and fully computer controlled using Wave Synthesizer. As the number of tests to be carried out is voluminous and in order to save time for testing, simultaneous testing of different configurations were aimed at without sacrificing the quality of testing. The flume of 2m width was partitioned longitudinally into three parts each of width of 0.66 m.

In the present experimental program, the wave elevation, wave run-up, pressures and forces on the structures as well as the velocity before and after the Green belt were measured using a set of instruments in the wave flume. The host computer that is used for controlling the wave maker is also used for acquiring the response from the different instruments used in this study. Then the calibration coefficients for each instrument have been directly input into the data collection software for directly obtaining the physical quantities. The calibration of all the instruments is done for each set of experiments to minimize the calibration errors in the experiments.

Propeller type velocity meters were used to measure the velocity on the upstream and downstream of the Green belt for the tests in the open channel. The wave probe used for the present tests comprises of two thin, parallel stainless steel electrodes. When immersed in water, the change in the conductivity of the instantaneous water column between the two electrodes is measured. This change is proportional to the variation of the water surface elevation between the electrodes. A beam type single component force transducer was used to measure the inline wave force on the model structure in the wave flume. The load cell had a maximum capacity of 200 N with an accuracy of 0.1 N and had strain gauges in half-bridge configuration. Similar to the principle of the wave gauge, the run-up probe was fabricated to measure the run-up on the outer cylinder. The run-up probe consists of two parallel stainless steel wires of 1 mm diameter spaced 10 mm apart and are fixed at specified locations on the beach slope. When immersed in water, the electrodes measure the conductivity of the instantaneous water volume between them. The conductivity change is proportional to the variation in the water surface elevation. Static calibration of run-up probe has been carried out to obtain the calibration constants.

Test Procedure

The open channel tests were manually carried out by adjusting discharges and measuring flow depths using height gauges and velocities using vane type flow meters. The flow depths h_u and h_d and mean flow velocities V_u and V_d have been measured for all the test combinations. Each of the above tests has been repeated 3 times for ensuring repeatability of measurements and only the mean values have been taken for further processing. These measurements have been used to arrive at the f for various flow as well as vegetative parameters. Snap shots recorded during the tests are shown in Fig.5a. The pictures bring out the hydraulic gradients observed during the tests. The resistance to the flow due to the presence of vegetation is dependent on the gradient between upstream and downstream flows. In general, it is observed that higher D and BG results in a higher gradient, the details of which for all the tests carried out are reported and discussed later. In the present study, the first modal frequency, f_1, was obtained by free vibration tests conducted after fixing strain gauges in a half bridge on the root of the model vegetal stem.

In the case of the tests in the wave flume, all the test signals acquired through an amplifier were filtered through a 20Hz low pass filter to remove the sampling ripples. A Personal Computer was used for the generation of waves and for the simultaneous acquisition of signals from the sensor pick-ups. The electrical signals were acquired using quartz clock controlled sampling and converted to digital form using a 12bit A/D (Analog to Digital) converter. The signals from various instruments were acquired with a sampling frequency of 40Hz. Sufficient time gap was allowed between successive runs to restore calm water condition in the wave flume.

Initially, tests without the vegetal patches were carried out in each of the flume compartments. The run–up measurements have been carried out without the wall (used for pressure measurements) and the model building (used for force measurements). The tests with Cnoidal waves were carried out in two water depths of 0.9 and 1 m, The run-up, R_u was thus measured for both the cases i.e., presence and absence of vegetation in order to quantify the role of wave height on the run-up (R_u/H). In addition, to the measurement of pressures on a wall in absence and presence of vegetation, the tests on the measurement of forces due to Cnoidal waves on a structure positioned at a distance, G of 0.0B, 0.5B, 1.0B and 1.5B, from the shoreline/reference line that was carried out under the second phase of the wave flume experiments. A model structure of dimension, 0.2 m*0.2 m and height of 0.3 m was mounted on a cantilever type load cell.

The depth of water at the toe, h of the beach slope was maintained at 1m. The testing parameters for both waves and the vegetation are the same as that adopted for the tests with pressures as discussed earlier. The test set-up for the measurement of forces on the structure (in absence of vegetation and with Staggered configuration of vegetation for any two BG) for G/B = 0, 0.5, 1.0 and 1.5. Typical experimental set-up used for the tests in wave flume for measuring the wave forces on a model building is shown in Fig.4a. The conditions for which the forces acting on a model building were measured in presence and absence of vegetation are projected in Fig. 4b. The complete details of the experimental investigations carried out are concisely summarised in Fig.4c.

3. Vegetal resistance and resulting runup, pressure and force

3.1 Resistance of flexible emergent vegetation in steady uniform flow

From the literature it is observed that a number of authors have investigated the resistance characteristics of emergent vegetation in the past under steady uniform flow while a few

have also considered the flexibility of vegetation. However, a comprehensive study considering more appropriate modelling of vegetal flow interaction is found to be warranted. The present effort focuses on the effect of the flexibility of vegetation on the resistance offered to the flow. The flexibility, being more of a material property, should be directly related to the Young's Modulus *E* of the vegetal material as found from a standard bending experiment of a simply supported beam with point loads and without involving the flow parameters. Furthermore, rigidity is defined as a product of *E* and the moment of inertia *I*. By doing this, the indirect way of establishing *E* as done by some of the authors (Freeman 1997; Jarvela 2004) has been avoided. Further, the limitation of the validity of *E* or the empirical model being a function of un-deflected plant height and the depth of flow is overcome.

In the present flow vegetation interaction, the resistance to the fluid flow is considered to be characterised by a number of friction factors. The resistance coefficients that are in use are the *Manning's n*, *Darcy Weisbach friction factor, f* and the *Chezy's constant C*. There are also a few studies where the vegetal drag has been investigated. The Darcy *f* has been quantified in the past through measurements in open channel experiments (Unny and Kouwen, 1969; Petryk and Bosmajian, 1975; Chen, 1976 and Werth, 1997) using various vegetation models. In general, it may be noted that the interaction between vegetation and flow has not been modelled appropriately and the elastic characteristics of vegetation has not been given due consideration. However, the previous investigators reported that quantifying the resistance using *f* has several advantages such as (i) the flow being taken past enclosed / partially enclosed vegetal volumes, (ii) ease of measurements in the laboratory, (iii) possibility of quantification of wall effects in open channel, etc. As such, the present work aims to investigate the Darcy's *f and Manning's n* for various flow as well as vegetative parameters.

In the present study, the resistance is investigated with respect to Reynolds' number (*Re*), relative spacing (*SP/D*), reduced velocity (V_r) and Vegetation-Flow Parameter (VFP) of the vegetal patch. The vegetation-flow parameters considered in the present study not only accounts for the flexural rigidity of the vegetation but also for the width of the green belt *BG*, flow depth *h* and the diameter of the vegetation *D*. As experiments were carried out over a wide range of flow as well as vegetative parameters, determination of *f and n* irrespective of the depth of flow and the un-deflected plant height to stem diameter is made possible. However, herein the results on the variation of *f* alone are projected.

Determination and quantification of resistance due to Vegetation

Utilising the Bernoulli's equation, the loss of head due to friction can be determined as,

$$H_f = \frac{V_u^2 - V_d^2}{2g} + (h_u - h_d) \tag{7}$$

V, *h* and *g* in the above equations are defined earlier and the suffix *u* and *d* correspond to the respective variables on upstream and downstream of flow respectively. However, H_f in the above equation also includes the contribution of flume walls and the bed. The energy loss due only to vegetation $H_{f\,(veg)}$ may be calculated by deducting the energy losses due to side and bottom walls $H_{f(wall)}$, from the total energy losses $H_{f(veg+wall)}$

$$H_{f\,(veg)} = H_{f(veg+wall)} - H_{f(wall)} \tag{8}$$

$$H_{f(veg+wall)} = \left\{ \left(\frac{V^2_{u(veg+wall)} - V^2_{d(veg+wall)}}{2g} \right) + \left(h_{u(veg+wall)} - h_{d(veg+wall)} \right) \right\} \tag{9}$$

$$H_{f(wall)} = \left\{ \left(\frac{V^2_{u(wall)} - V^2_{d(wall)}}{2g} \right) + \left(h_{u(wall)} - h_{d(wall)} \right) \right\} \tag{10}$$

$$H_{f(veg)} = \left\{ \left(\frac{V^2_{u(veg+wall)} - V^2_{d(veg+wall)}}{2g} \right) + \left(h_{u(veg+wall)} - h_{d(veg+wall)} \right) \right\} - \left\{ \left(\frac{V^2_{u(wall)} - V^2_{d(wall)}}{2g} \right) + \left(h_{u(wall)} - h_{d(wall)} \right) \right\} \tag{11}$$

Herein, $V_{u(veg+wall)}$ is upstream velocity measured in the presence of vegetation, $V_{u(wall)}$ is upstream velocity measured in the absence of vegetation; $h_{u(veg+wall)}$ is depth of flow upstream of the vegetation; $h_{u(wall)}$ is depth of flow at the upstream location in the absence of the vegetation; $V_{d(veg+wall)}$ is velocity measured with vegetation on the downstream; $V_{d(wall)}$ is velocity measured without vegetation on the downstream; $h_{d(veg+wall)}$ is depth of flow down stream of the vegetation; $h_{d(wall)}$ is depth of flow downstream in the absence of the vegetation; $V_{d(veg+wall)}$ is velocity measured with vegetation on the downstream**.** It is to be noted that the above approach consistently eliminates the presence of wall effects in the measurements, irrespective of the location of upstream and downstream measurement points. A similar exercise has been carried out for the Manning's *n,* however, the details of which are not reported. Snap shots recorded during the tests are shown in Fig.5. The pictures bring out the hydraulic gradients observed during the tests.

Friction factors and their quantification

Froude model law is usually employed for studying open channel hydraulics. However, it the dependence of *f* with respect to *Re* is considered up-front for the purpose of validation of the results with that in the literature. Jarvela (2002) has measured the *f* for sedges for a wide range of *Re* in a flow depth of 0.2m, the results of which are superposed with the present results for *f,* for flow depth ranging between 0.19m and 0.2m, in Fig.6a. This comparison validates the measurements with that of Jarvela (2002) in the range of *Re* considered. The above said variation have been grouped for three different values of h_{avg}/R_h of 1.5, 1.7 and 1.9 and superposed in Fig.6b, suggesting that the *f* has a strong correlation with the non-dimensional flow. From the results it is seen that the *f* is sensitive to the variation h_{avg}/R_h for lower *Re*. The friction factor appears to increase drastically by about 50%-100% as the h_{avg}/R_h increases by about 100%.

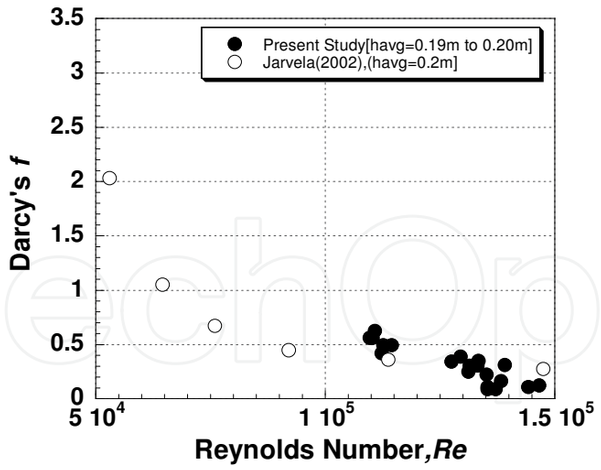

Fig. 6 a. Comparison of variation of *f* with *Re*-(present results with Jarvela(2002)

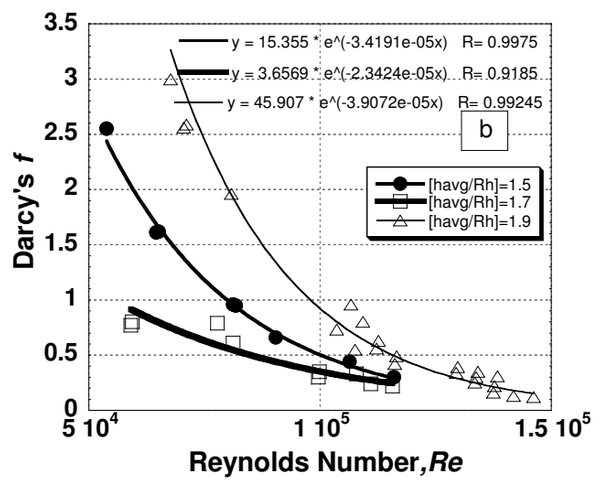

Fig. 6 b. Variation of *f* with Re as a function of relative flow depth.

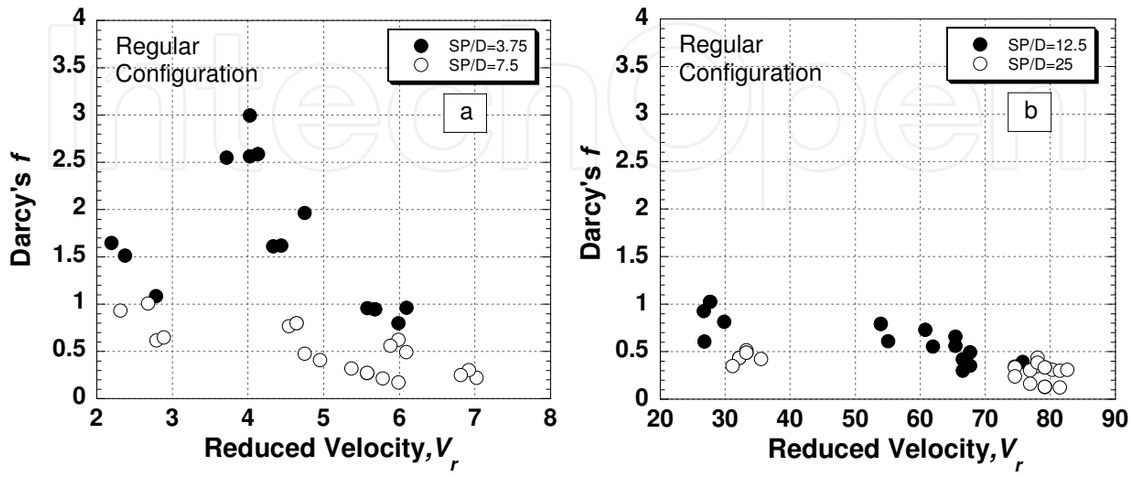

Fig. 7. Variation of Darcy's *f* with V_r for different ranges of *SP/D* in tandem configuration.

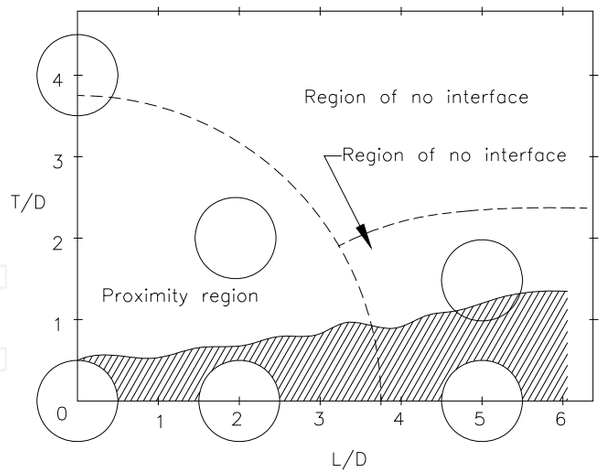

Fig. 8. Interface Region in flow around cylinders (after Zdravkovich and Medeiros, 1991).

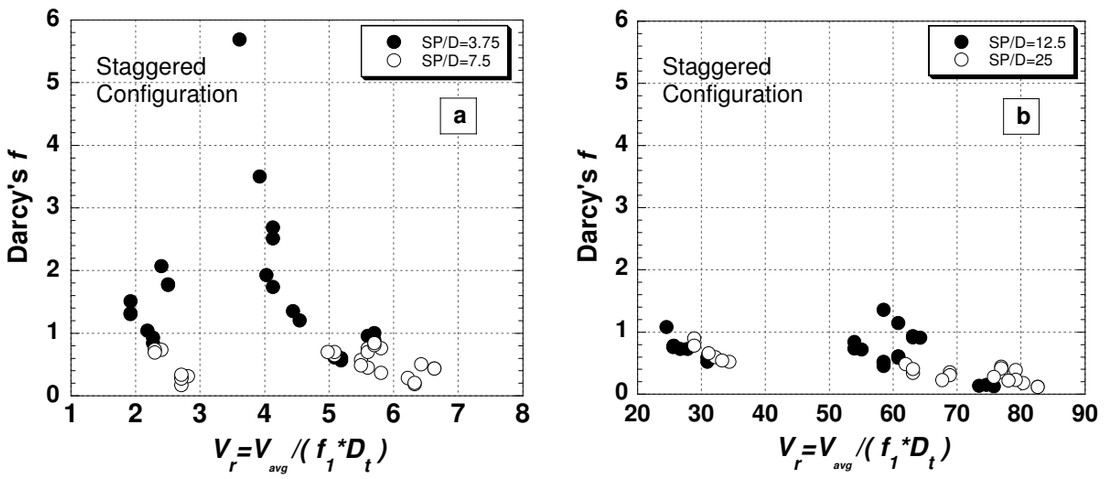

Fig. 9. Variation of Darcy's f with V_r for different ranges of SP/D in Staggered configuration.

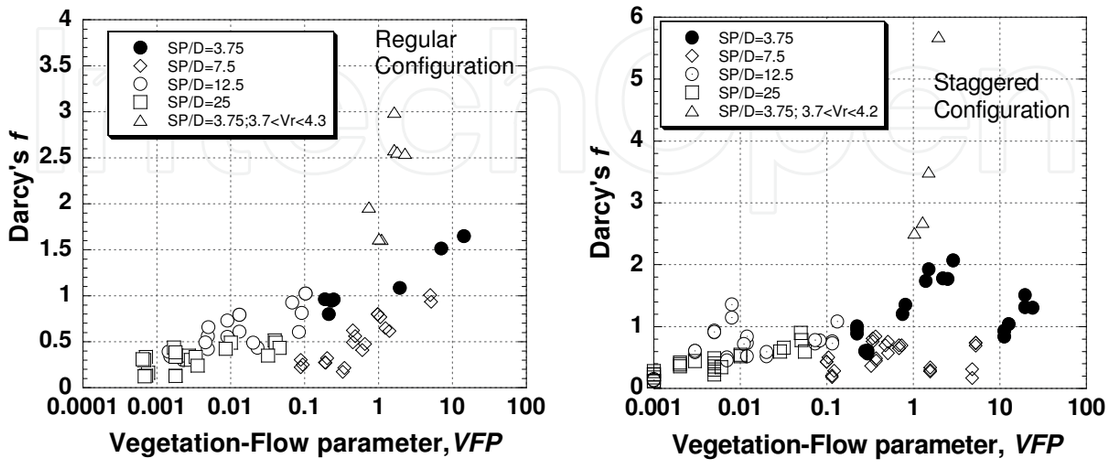

Fig. 10. Variation of Darcy friction factor f with Vegetation-Flow Parameter for different ranges of SP/D in Tandem configuration.

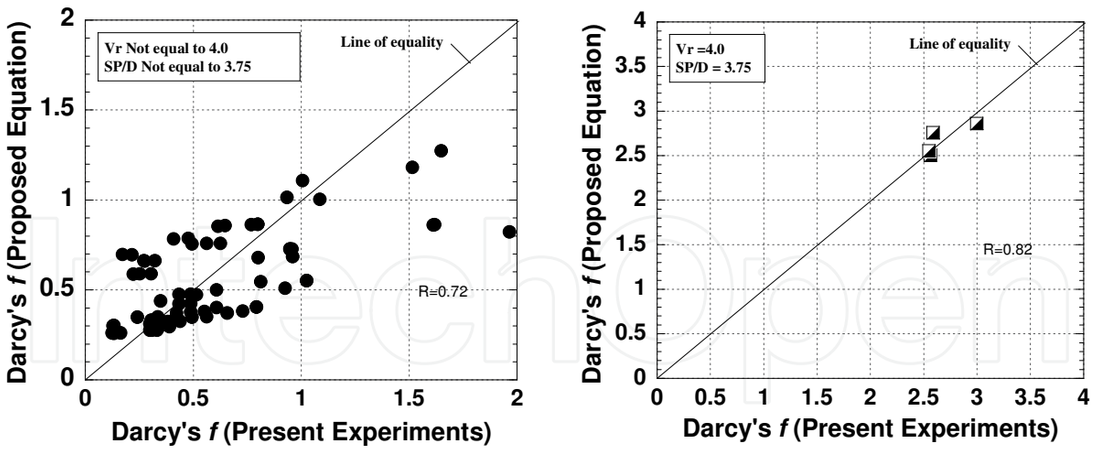

Fig. 11. Darcy's f – Comparison of present proposed equation with present measurements. When proximity and wake effects are presents, large friction is observed.

Proposed empirical formula (no wake and proximity effects)	Proposed empirical formula (with wake and proximity effects)
$f_{\mathrm{Re}g} = 1.005 * \left(\frac{EI*(BG/D)}{\rho HV^2 l^3 (SP/D)}\right)^{0.1680} \left(\frac{V_{avg}}{\sqrt{gh_{avg}}}\right)^{0.2479}$	$f_{\mathrm{Re}g} = 7.488 * \left(\frac{EI*(BG/D)}{\rho HV^2 l^3 (SP/D)}\right)^{-0.2654} \left(\frac{V_{avg}}{\sqrt{gh_{avg}}}\right)^{1.099}$
$f_{Stg} = 0.463 * \left(\frac{EI*(BG/D)}{\rho HV^2 l^3 (SP/D)}\right)^{0.0789} \left(\frac{V_{avg}}{\sqrt{gh_{avg}}}\right)^{-0.5211}$	$f_{Stg} = 0.196 * \left(\frac{EI*(BG/D)}{\rho HV^2 l^3 (SP/D)}\right)^{1.4136} \left(\frac{V_{avg}}{\sqrt{gh_{avg}}}\right)^{-3.098}$
$n_{\mathrm{Re}g} = 0.0422 * \left(\frac{EI*(BG/D)}{\rho HV^2 l^3 (SP/D)}\right)^{0.1332} \left(\frac{V_{avg}}{\sqrt{gh_{avg}}}\right)^{-0.2217}$	$n_{\mathrm{Re}g} = 0.229 * \left(\frac{EI*(BG/D)}{\rho HV^2 l^3 (SP/D)}\right)^{0.01812} \left(\frac{V_{avg}}{\sqrt{gh_{avg}}}\right)^{1.26}$
$n_{zz} = 0.0466 * \left(\frac{EI*(BG/D)}{\rho HV^2 l^3 (SP/D)}\right)^{0.0641} \left(\frac{V_{avg}}{\sqrt{gh_{avg}}}\right)^{-0.0865}$	$n_{zz} = 0.0279 * \left(\frac{EI*(BG/D)}{\rho HV^2 l^3 (SP/D)}\right)^{0.8016} \left(\frac{V_{avg}}{\sqrt{gh_{avg}}}\right)^{-1.554}$
$E_{L(Reg)} = 0.4369 * \left(\frac{EI*(BG/D)}{\rho h_u V_{avg}^2 l^3 (SP/D)}\right)^{0.2038} \left(\frac{V_{avg}}{\sqrt{gh_{avg}}}\right)^{0.5413}$	$E_{L(Reg)} = 4.25 * \left(\frac{EI*(BG/D)}{\rho h_u V_{avg}^2 l^3 (SP/D)}\right)^{0.2357} \left(\frac{V_{avg}}{\sqrt{gh_{avg}}}\right)^{3.0015}$
$E_{L(Stg)} = 0.171 * \left(\frac{EI*(BG/D)}{\rho h_u V_{avg}^2 l^3 (SP/D)}\right)^{0.1028} \left(\frac{V_{avg}}{\sqrt{gh_{avg}}}\right)^{-0.3949}$	$E_{L(Stg)} = 0.099 * \left(\frac{EI*(BG/D)}{\rho h_u V_{avg}^2 l^3 (SP/D)}\right)^{1.2722} \left(\frac{V_{avg}}{\sqrt{gh_{avg}}}\right)^{-1.7077}$

Table 2. Proposed formula for f, n and E_L

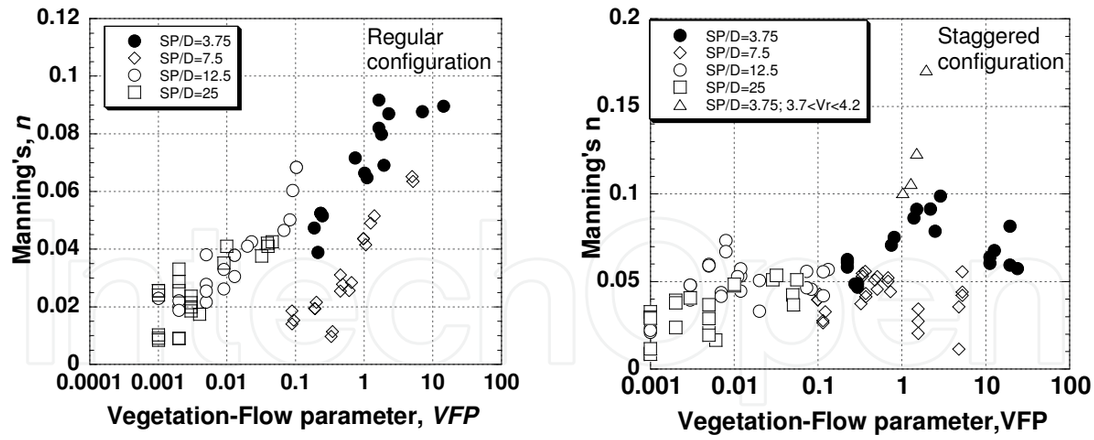

Fig. 12. Variation of Manning's *n* with Vegetation-Flow Parameter for different ranges of *SP/D*.

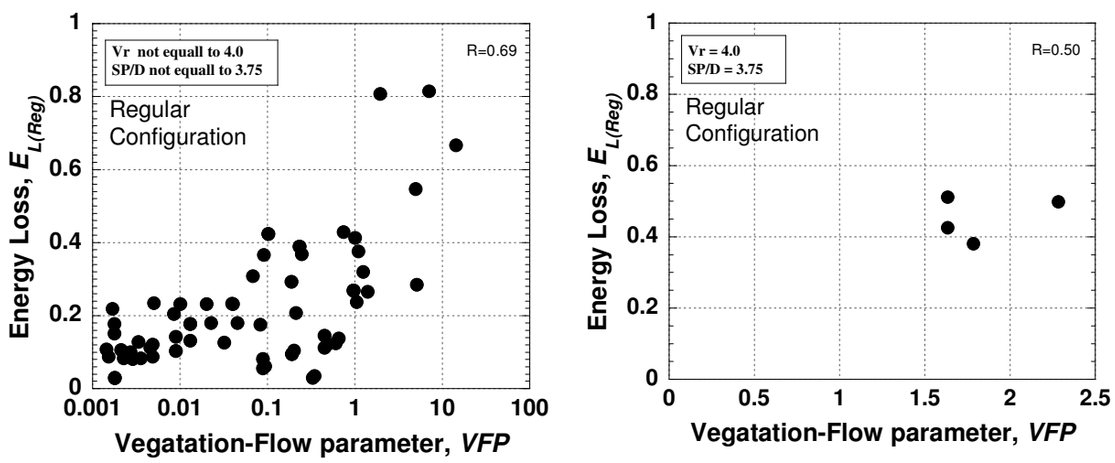

Fig. 13. Representation of Manning's *n* with Vegetation-Flow Parameter for different ranges of *SP/D*.

Dependence of 'f' on Reduced Velocity 'V_r' and Relative Spacing 'SP/D'

Considering the number of parameters involved in the resistance offered by vegetal stems needs an in-depth understanding of the possible non-dimensional groups that could dictate specific regions of the flow-vegetation interaction. Detailed analysis indicate that the reduced velocity (V_r) and vegetation-flow parameter to be important parameters.

The variation of *f* with Reduced Velocity V_r for different ranges of Relative spacing, *SP/D* is investigated in Fig.7 for tandem configuration of vegetation**.** The range of experimental data for V_r is 2.0< V_r <8.0 and 20< V_r <90. It is found that the *f* has a strong correlation with V_r and *SP/D*. The *f* is consistently close to or less than 1.0 for values of V_r other than about 4.0 and *SP/D* other than 3.75. The *f* reduces with an increase in the V_r for *SP/D* greater than 3.75. For *SP/D* =3.75, the *f* is found to increase for V_r in between 3 and 4, thereafter, the *f* in general is found to decrease. Two distinct processes that have been observed in the experiments are responsible for this distinct behaviour of *f*. These are the Wake and Proximity induced vibrations of the model stems. The Wake induced vibrations of Vortex Induced Vibrations (VIV) is expected to have a significant effect in the flow-vegetation

interaction and care has been taken to keep the elasticity and flow variables with in the range of requisite non-dimensional parameters, the most important being the Reduced Velocity, V_r. In the present experimental parameters, V_r is defined as $V_{avg}/(f_1 D_t)$ as described earlier. Since the *Strouhal Number,*($S_t = Df_s/V_{avg}$) that is about 0.25, does not appear in the definition of V_r, it is expected that "*lock-in*" (matching of Vortex shedding frequency with the natural frequency of the model vegetal stem) will take place around V_r =4.0. When the lock-in occurs, the vortex street downstream of any structural member will be oscillated with the most possible structural vibrations. It may be concluded that, higher the structural vibrations, better the energy dissipation leading to an increase in *f*. This is observed in this case to be as high as 200% more than the non lock-in regime resulting in values of *f* as high as 3.0. However, the same is not observed for other values of *SP/D* considered in the study. This can be explained with reference to the proximity effect. The proximity effect is the effect of presence of neighbouring cylinders in the flow, in the transverse direction. The combined interaction of Proximity and Wake induced oscillations has been investigated by Zdravkovich and Medeiros (1991). For benefit of the readers, a figure describing this effect is reproduced in Fig.8 based on the original publication**.** It is seen that, as long as the *SP/D* is about 3.8, the combined Proximity and Wake effects will be present in the structural response. Hence, we obtain the highest measured *f* for the combination of *SP/D* =3.75 and V_r ~4.0. It is to be noted that this refers to densely spaced vegetation. In the experiments, this is the lowest value of relative spacing that has been considered. Specific mention needs to be made to the fact that, closer spacing may not be possible in real situations pertaining to vegetation in flow or Greenbelt. In the case of sparsely spaced vegetation, for other *SP/D* (7.5, 12.5 & 25.0) and V_r >20, the *f* is found to be consistently around or less than 1.0, which is obvious as no lock-in or a proximity effect is expected for this combination of parameters.
It is usually expected that the staggered placement of vegetal stems would be more effective in offering resistance to flow (Fig.9). The staggered placement is seen to give about 20% improved resistance when compared to tandem configuration.

Vegetation Flow Parameter 'VFP' and its effect on resistance

Relating *EI, BG, l,* V_{avg}, ρ, h_{avg} and *SP/D*, the Vegetation-Flow Parameter is defined as,

$$\mathrm{VFP} = \left(\frac{EI * (BG / D)}{\rho h_u l^3 V_{avg}^2 (SP / D)} \right) \tag{12}$$

The plot showing variation of *f* with *VFP* is shown in Fig.10 for both tandem and staggered configuration. For lower rigidity and higher *SP/D*, the *f* is less than 1.0. A general trend of higher *f* for higher *VFP* is clearly visible, meaning that, higher Relative Rigidity will provide higher resistance. For the range of up to *VFP* = 0.8, the *f* value is always less than 1.0. The critical range of *VFP* is about 1.0. At this *VFP*, very high values of *f* (up to above 3) may be encountered due to the combined effect of Wake and Proximity induced oscillations. Further beyond *VFP* =1, an increasing trend in *f* is once again observed. For a maximum value of *VFP* ~15, the maximum *f* value of 1.5 is observed. In the critical range of *VFP* =1, a steep increase in *f* with *VFP* is observed from 1.5 to 3.0 with a maximum *f* occurring at *VFP* ~1.5. The forgoing discussion confirms that the new vegetal parameter *VFP*, is able to reasonably scale the structural rigidity with reference to the vegetation and flow parameters. Hence this shall be used as a key parameter in greenbelt design.

Empirical relationship for f

The aforementioned discussion indicates that the vegetal resistance or drag depends itself on many variables. With the results presented above as the background, a multiple regression analysis with suitable variables provides the most useful relationship which could be used is applications. For this purpose the *Fr* and *VFP* were selected. The *Fr* determines hydraulic regime of the flow while the *VFP* determines the hydro-elastic scale. Hence, the parameters shall appear in the relationship. However, the data was split into two categories. The first category pertaining to all the data except the range of *SP/D* =3.75 and V_r ~4.0. The second category pertaining to the range of *SP/D* =3.75 and V_r ~4.0. These classifications were necessary to avoid unwanted scatter in the fit and provide best possible regression coefficient. The new empirical equations thus obtained are given in eqs.24 and eq.25 for the two categories of data.
While $SP/D \neq \sim 3.75$ and $V_r \neq \sim 4.0$

$$f_{tandem} = 1.005 * \left(\frac{EI * (BG / D)}{\rho h_u V_{avg}^2 l^3 (SP / D)} \right)^{0.1680} \left(\frac{V_{avg}}{\sqrt{g h_{avg}}} \right)^{0.2479} \tag{13}$$

While $SP/D = \sim 3.75$ and $V_r = \sim 4.0$

$$f_{tandem} = 7.488 * \left(\frac{EI * (BG / D)}{\rho h_u V_{avg}^2 l^3 (SP / D)} \right)^{-0.2654} \left(\frac{V_{avg}}{\sqrt{g h_{avg}}} \right)^{1.099} \tag{14}$$

The above relationships represent the data within a maximum standard deviation of 10%. These relationships may be used with in the range of $0.25 \leq F_r \leq 0.60$. Further, it is observed that all the parameters are physically reasonably related to the *f*. In order to ascertain the quality of the fit presented above, the relationship between measured and predicted *f* values for a given set of experimental parameters for the above equations are presented in Fig.11. It is once again noticed that most of the data fall around the line of equality for both the data ranges. It is proposed that the above empirical models may be used in practical application of Green belt / Bio shield.

Manning's coefficient 'n' for vegetal patch.

Similar to *'f'*, the Manning's n could also be studied in terms of *Re* and Reduced Velocity V_r, and similar discussion could be made. Following the procedures adopted for *f*, the dependence of Manning's *n* with the newly proposed Vegetation Flow Parameter is brought out in Fig. 12. The comparison shows an excellent correlation for any given *SP/D* (7.5-25). The Manning's *n* varies between 0.01 and 0.065. However, for the case, where proximity effect is present, the minimum Manning's *n* observed is about 0.04 which increases to about 0.09 towards the experimental regime of wake effects. The wake effects are not very much pronounced in the case of Manning's *n* in tandem configuration. It is observed that for the range of Vegetation Flow Parameter studied, the Manning's *n* has a linear relationship with the Vegetation Flow Parameter. Similar to *'f'*, the newly proposed empirical relationship for Manning's *n* in terms of F_r and *VFP* are given in Table.2. These relationships represent the data within a maximum standard deviation of 12%. These relationships may be used with in the range of $0.25 \leq Fr \leq 0.60$. Further, it is observed that all the parameters are physically related to the *n.*

The Manning's n has been computed for staggered configuration from the experimental measurements using the same approach outlined earlier. The superiority the staggered configuration over the tandem configuration is brought out once again in the above figure. The increase in n when the proximity and wake effect are present is about 50-60% occurring at the value of *VFP* of about 1.0. For the other scenarios, a 20-30% increase is evident. Once again, the empirical relationships for evaluating the 'n' value for staggered configuration are given in Table.2. It is found that these relationships are better than that proposed by Freeman *et al*. (2000) as demonstrated by Noarayanan et al. (2009). It is also demonstrated that the presently proposed vegetal parameter, VFP, is superior to the earlier vegetal parameters.

3.2 Relationship of energy loss with vegetation-flow parameter

The f and n are the most important parameters for vegetal drag or head loss. However, their direct use in the design of Greenbelt is not quite straightforward. One needs to have a fair understanding of the energy loss and its direct relation to the vegetal and flow parameters in order to perform a design calculation for Green belt. To this end, the normalized Energy Loss $E_{L(Reg)}$ and $E_{L(Stg)}$, with reference to the upstream energy content is considered as against the Vegetation Flow Parameter *VFP* so that a direct relation between the Greenbelt parameters and drop in energy within the Greenbelt may be obtained. The variations of $E_{L(Reg)}$ as a function of *VFP* for tandem and staggered configurations are displayed in Figs.13a and Fig.13b respectively. The $E_{L(Tan)}$ is found to increase from about 0.1 at *VFP* ~0.001 to 0.8 at *VFP* 1.5. It is to be recalled that the maximum f and n have been observed at the same value of *VFP* as reported in earlier figures. Beyond *VFP* =1.5, the $E_{L(Tan)}$ reduces and is about 0.30 at *VFP*~15. Furthermore, the effects of wake and proximity interactions are once again brought out in the $E_{L(Tan)}$ also as the variation of $E_{L(Tan)}$ for *SP/D*=3.75 show a clearly superior performance than the other combinations. Similar trend is observed in the Energy Loss with *VFP* for the vegetations in the Staggered configuration. The energy loss is about 150 – 200% more (0.4 – 0.9) for *SP/D*=3.75 while, the range of $E_{L(Tan)}$ for higher *SP/D* is between 0.05-0.4. The mechanisms of wake and proximity effects are discussed earlier and hence are not repeated here.

An attractive proposition is to obtain a direct relationship between $E_{L(Reg)}$ and the independent parameters concerning the flow and Greenbelt. Once again, the multiple regression procedure is extended for $E_{L(Reg)}$ and other parameters. However, in this case, to keep the relationship simple only F_r and *VFP* are used in the regression procedure.

While $SP/D \neq \sim 3.75$ and $V_r \neq \sim 4.0$

$$E_{L(Reg)} = 0.4369 * \left(\frac{EI * (BG / D)}{\rho h_u V_{avg}^2 l^3 (SP / D)} \right)^{0.2038} \left(\frac{V_{avg}}{\sqrt{g h_{avg}}} \right)^{0.5413} \tag{15}$$

While $SP/D = \sim 3.75$ and $V_r = \sim 4.0$

$$E_{L(Reg)} = 4.25 * \left(\frac{EI * (BG / D)}{\rho h_u V_{avg}^2 l^3 (SP / D)} \right)^{0.2357} \left(\frac{V_{avg}}{\sqrt{g h_{avg}}} \right)^{3.0015} \tag{16}$$

Similar relationship for the Staggered configuration are presented below to obtain a direct relationship between $E_{L(Stg)}$and the independent parameters concerning the flow and

Greenbelt. Once again, the multiple regression procedure is extended for $E_{L(Stg)}$and other parameters, yielding the following relationships.
While $SP/D \neq \sim 3.75$ and $V_r \neq \sim 4.0$

$$E_{L(Stg)} = 0.171 * \left(\frac{EI * (BG / D)}{\rho h_u V_{avg}^2 l^3 (SP / D)} \right)^{0.1028} \left(\frac{V_{avg}}{\sqrt{g h_{avg}}} \right)^{-0.3949} \quad (17)$$

While $SP/D = \sim 3.75$ and $V_r = \sim 4.0$

$$E_{L(Stg)} = 0.099 * \left(\frac{EI * (BG / D)}{\rho h_u V_{avg}^2 l^3 (SP / D)} \right)^{1.2722} \left(\frac{V_{avg}}{\sqrt{g h_{avg}}} \right)^{-1.7077} \quad (18)$$

3.3 Application of the model

A typical sample application of the present empirical mod*e* for a real field situation is demonstrated herein based on the newly proposed empirical relationship for $E_{L(Reg)}$ eq.16. The different parameters in the field obtained based on design requirements are provided in Table.3.The procedure used for obtaining the values in the above table is highlighted below.

Design Example

Design a green belt for a storm surge of 5m, in such a way that the surge height may be reduced by half on its lee side. The available width of beach may be taken to be 150m. Assume an *Fr* of 0.4 for the flow induced by surge of height of 5m, assumed to reduce on downstream to 2.5m. The width of green belt has to be less than or equal to 150 m.

The following are the assumptions:

1. Froude number is assumed to be 0.40 (can be obtained from the ingress velocity in the field).
2. Fully grown diameter beachfront vegetation is taken to be 0.4m and (2/3) of this diameter is used for design.
3. Vegetal parameters: E = 9.0 GPa (common Oak) to 18.5 GPa (Red Mangroves)
   ρ = 1100 kg/m3
   SP/D = 6.0 (for design)
   = 4.0 (for fully grown condition)

Calculation procedure:

Using the above data and assumptions, the variables in *VFP* are derived and applied in eq.12. The design $E_{L(Reg)}$ is obtained based on given data as 0.36 with a factor of uncertainty of 1.5. Finally, the green belt parameter *BG* is obtained from eq.15 and reported in the above table.
The attractiveness of eq.15 and the usefulness of the newly proposed *VFP* are brought out by the above design example. While the said equation is simple to use, it relates the progressive loss of energy within the Greenbelt as a function of *VFP* which contains the vegetal parameters, flow parameters and greenbelt parameters. Hence, for a required E_l, one could obtain the *BG* and *SP/D*. Secondly; since $E_{L(Reg)}$ is proportional to *VFP* we get a higher *BG* for a weaker species (like Oak) and lesser *BG* for a stronger species (like Mangrove) which is physically understandable. In other words, realistic design of Greenbelt is possible with the proposed equations which include the *VFP* parameter.

Properties	Oak tree[Light]	Casurina[Medium]	Mangrove[Heavy]
E	9Gpa	14Gpa	18.5Gpa
Dt	0.267 m	0.267 m	0.267 m
λ	1	1	1
f_1	0.3037	0.37	0.43
Vr	51.9	41.6	36.2
SP/Dt	6	6	6
RR	3.87	4.02	3.98
Design *BG*	**120 m**	**80 m**	**60 m**

Table 3. Design example-Comparison of design for various species.

3.4 Engineering benefits of vegetation on beaches

This part of the chapter is purposed in bringing out the beneficial effects of vegetation on beaches. It is common to presume that the presence of vegetal patches on beach fronts would help protect the beach. Numerous studies have been reported in the literature, wherein, the friction factors or drag coefficient due to vegetation is reported.

Pressure reduction on a wall protected by vegetal patch

The variation of measured non-dimensional pressure, $P^* = p_{max}/H$ during the impingement of wave, with vegetal parameter (α) and relative water depth (h_s/gT^2). Herein, the vegetal parameter (α) is defined as ($BG{\cdot}SP/D^2$). Typical plots showing the variations of dimensionless pressure along the vertical wall, for $h_s/(gT^2) = 0.0004$ and various α, are shown in Fig. 14. As the wall is exposed to shallow water waves the variations in the dynamic pressures along its depth is found to be insignificant for any of the two configurations considered. Further, the results indicate, that the pressures at all the three wall ports reduce in presence of vegetation. Note that the pressure reduces from about 10% to a maximum of about 35%. Further, the pressure reduction is observed to be almost twice for staggered vegetation. The pressures measured by the pressure port near the free surface at $z/h_s = -0.05$ is lower than that of the middle pressure transducer, while that close to the bottom experiences the least pressure. However a pressure reduction at the top transducer is not expected. Note that the top pressure port is close to the free surface and above the lowest location of the wave crest, leading to a pressure relief in this region as the wave runs up the wall. Hence, the trend in pressure variation along a wall as reported. Typical variations of P^* versus α for $z/h_s = -0.45$ and two values of $h_s/(gT^2)$ shown in Fig. 15 indicate that the least pressure is experienced by wall-fronted by staggered vegetation. The variation of P^* with $h_s/(gT^2)$ for all the pressure port locations and $\alpha = 375$ in Fig. 16 shows that it decreases with an increase of $h_s/(gT^2)$ as pressure exerted by long waves is higher, which was found consistent for the other α tested.

The results on the wall pressures revealed that the staggered configuration has a clear advantage because the pressure reduction is found to be almost twice. This is due to the continuous dissipation from the sea-front to the lee-side of vegetation caused by staggered vegetation which is absent for tandem vegetation. This aspect was confirmed by Kothyari *et al.* (2009) through experiments in open channel flow. It is observed that the placement of vegetation has a major role in drag offered by the stems in the flow. As a result more energy is dissipated in case of staggered placement, leading to reduced pressures.

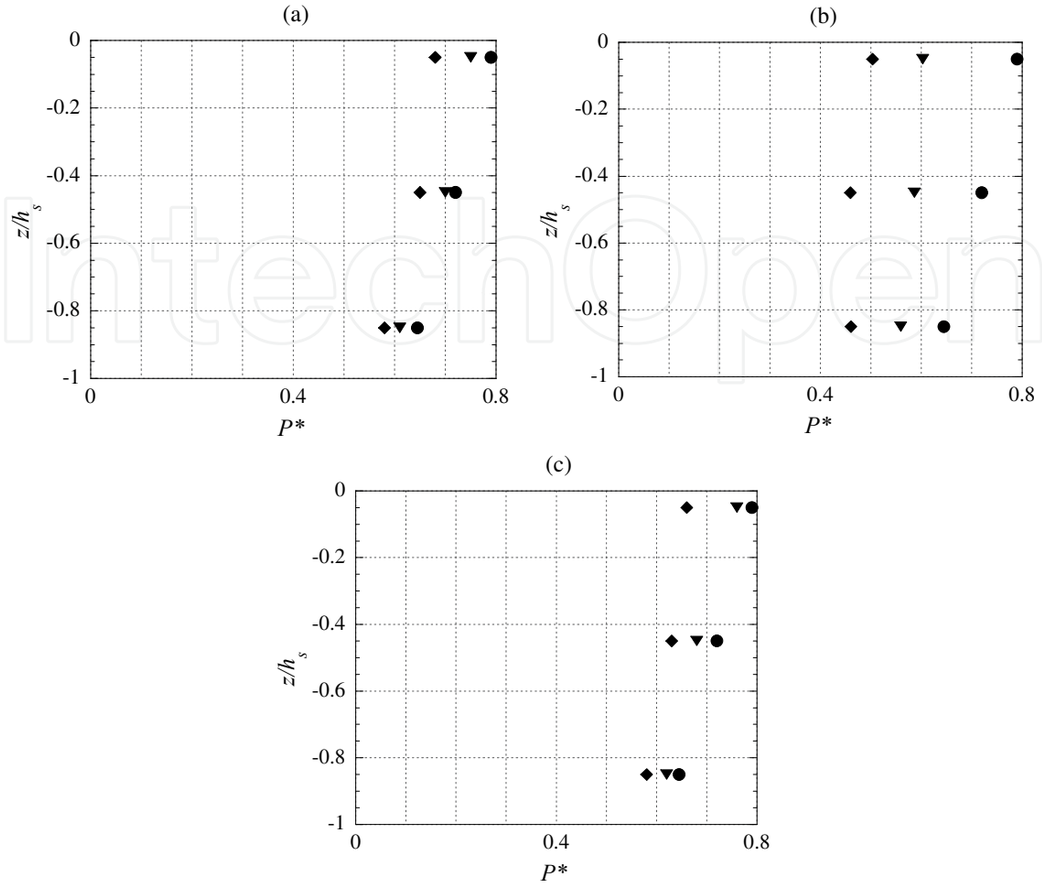

Fig. 14. Variation of $P^* = P_{max}/H$ with z/h_s for H=0.11 m and h_s/gT^2=0.0004 with (●) No, (♦) staggered and (▼) tandem vegetation for α = (a) 1041, (b) 2083, (c) 2604

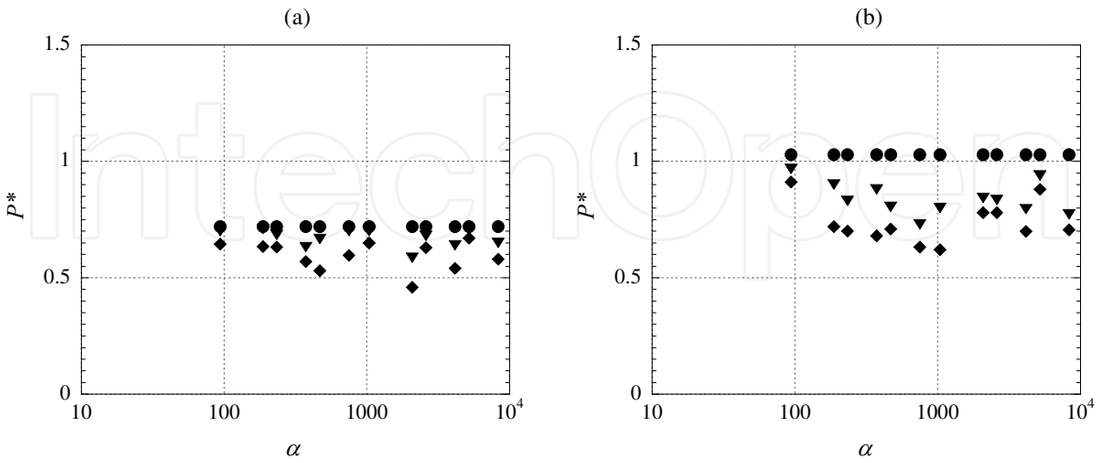

Fig. 15. Variation of $P^* = P_{max}/H$ with α at z/h_s =–0.45 for h_s/gT^2 = (a) 0.0004, (b) 0.0001 (with (●) No, (♦) staggered and (▼) tandem)

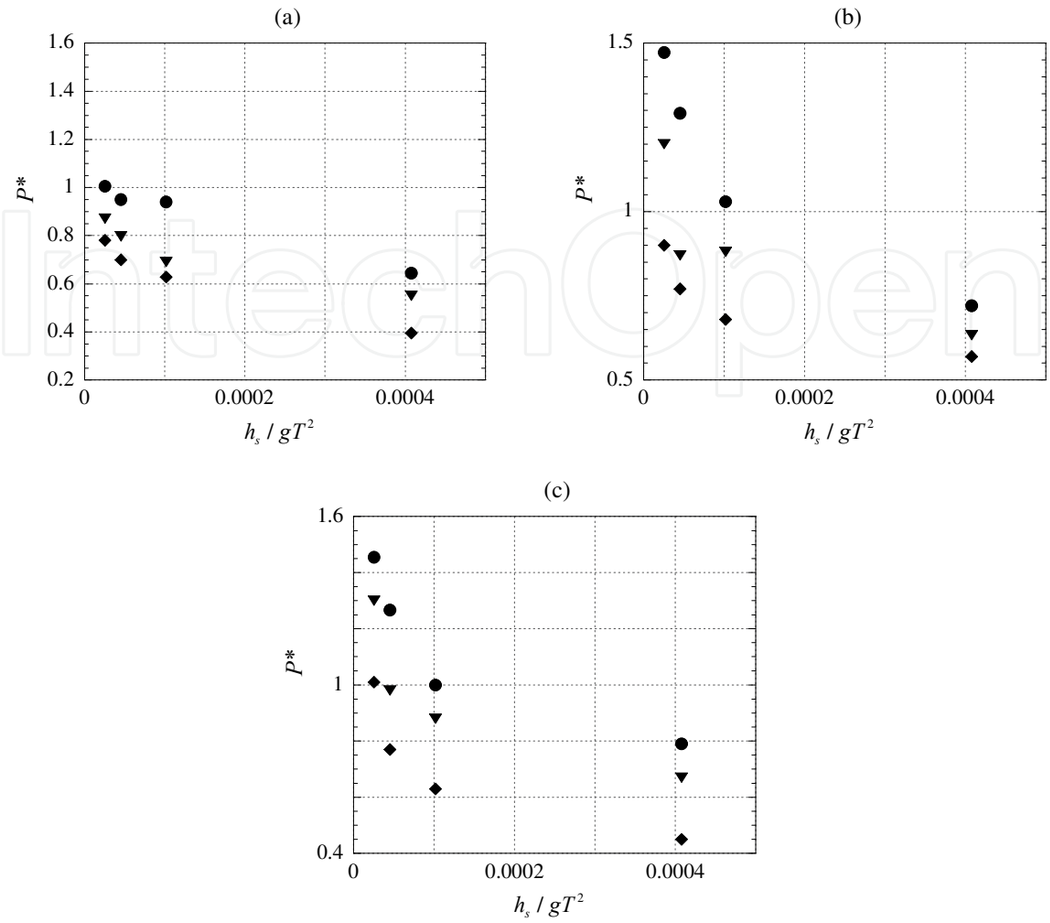

Fig. 16. Variation of $P^* = P_{max}/H$ with h_s/gT^2 for α =375 and z/h_s = (a) –0.85, (b) –0.45, (c) –0.05, (with (●) No, (♦) staggered and (▼) tandem)

The parameter α appears to be reasonable to quantify the effect of vegetal placement. Increasing SP/D corresponds to an increase in the spacing between the individual stems within the green belt, leading to an inferior green belt, for which BG is wider. It was observed that a dense vegetal placement reduces pressure as $\alpha < 750$ with the percentage reduction in pressure increase with an increase in the green belt width by about 25 to 30%. For $\alpha > 750$, i.e. a larger spacing between the stems, a marginal drop in the mean percentage of pressure reduction of about 22 to 30% was observed. From the time histories recorded by the centre pressure sensor, equations through a regression analysis for pressure reduction due to staggered and tandem vegetations were obtained as

$$P_{StaggeredVeg} = 1.244\left(\frac{h_s}{gT^2}\right)^{-0.3232} \cdot \alpha^{0.0062} \tag{19}$$

$$P_{TandemVeg} = 0.092\left(\frac{h_s}{gT^2}\right)^{-0.4635} \cdot \alpha^{0.0874} \tag{20}$$

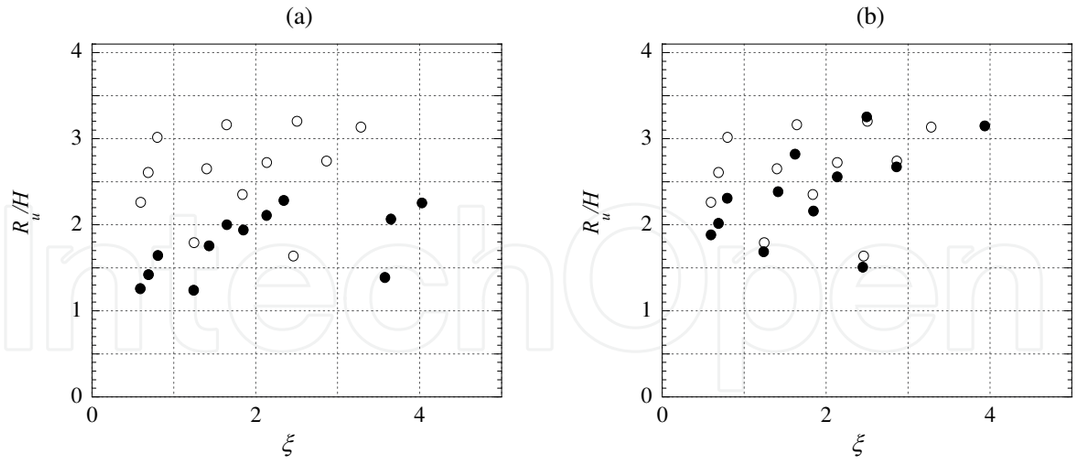

Fig. 17. Variation of R_u/H with ξ for α = (a) 375, (b) 750, Symbols (with (●) No, (♦) staggered and (▼) tandem

Run up on beaches fronted by vegetal patch

The tests on the measurement of wave run-up on the slope were conducted only for staggered vegetation for which the pressures on the lee-side wall were less than that for tandem vegetation, as reported above. Only typical results on the variations of R_u/H with ξ in presence and absence of vegetation for two values of α are shown in Fig. 17 for *BG*= 1 m. It is seen that R_u/H increases with an increase in ξ. The plots also show variations of wave run-up on a slope without vegetation. A significant reduction of run-up is observed in presence of staggered vegetation.

The non-dimensional run-up increases linearly as the surf similarity parameter increases. The percentage reduction of run-up due to waves in the presence of the vegetation is about 40% for the higher surf similarity parameter. Even if the width of vegetation with respect to the water depth is less, the attenuation is dominant due to the flow passing through a medium of lower porosity. The R_u/H on the slope decreases in the presence of green belt, the rate of reduction being significant to an extent of about 60% for Cnoidal waves for higher values of ξ, that is, for long waves propagating over a slope. The tests with long waves exhibits that high degree of reduction in the run-up can be achieved even with sparse spacing (larger porosity) provided the greenbelt is wider. For larger width of green belt, the run-up is independent of the porosity, as shown using the *SP/D* parameter, of the vegetation. The percentage reduction of run-up is more for lesser *BG* of lesser porosity. The effect of vegetation is to reduce the R_u/H_s by about 40 %. This is valid for all the Vegetal parameter investigated.

Attenuation of forces on model buildings

Only salient results on the variations of dimensionless force, F^* (= $\left[\left(F_{\max}\right)/\left(0.5*\rho*g*H^2*B_s\right)\right]$) are presented herein in order to clearly bring out the prime aspects of attenuation of wave forces on typical model building fronted by vegetation. The variations of F^* with the vegetation-flow parameter *VFP* is plotted in Fig.18 for the value of α=375 and for *G/B* values of 0, 0.5, 1, and 1.5. To bring out clarity on the effect of vegetation, the results obtained for forces in its presence and absence are superposed. For the case *G/B*=0 (recall, G/B is gap

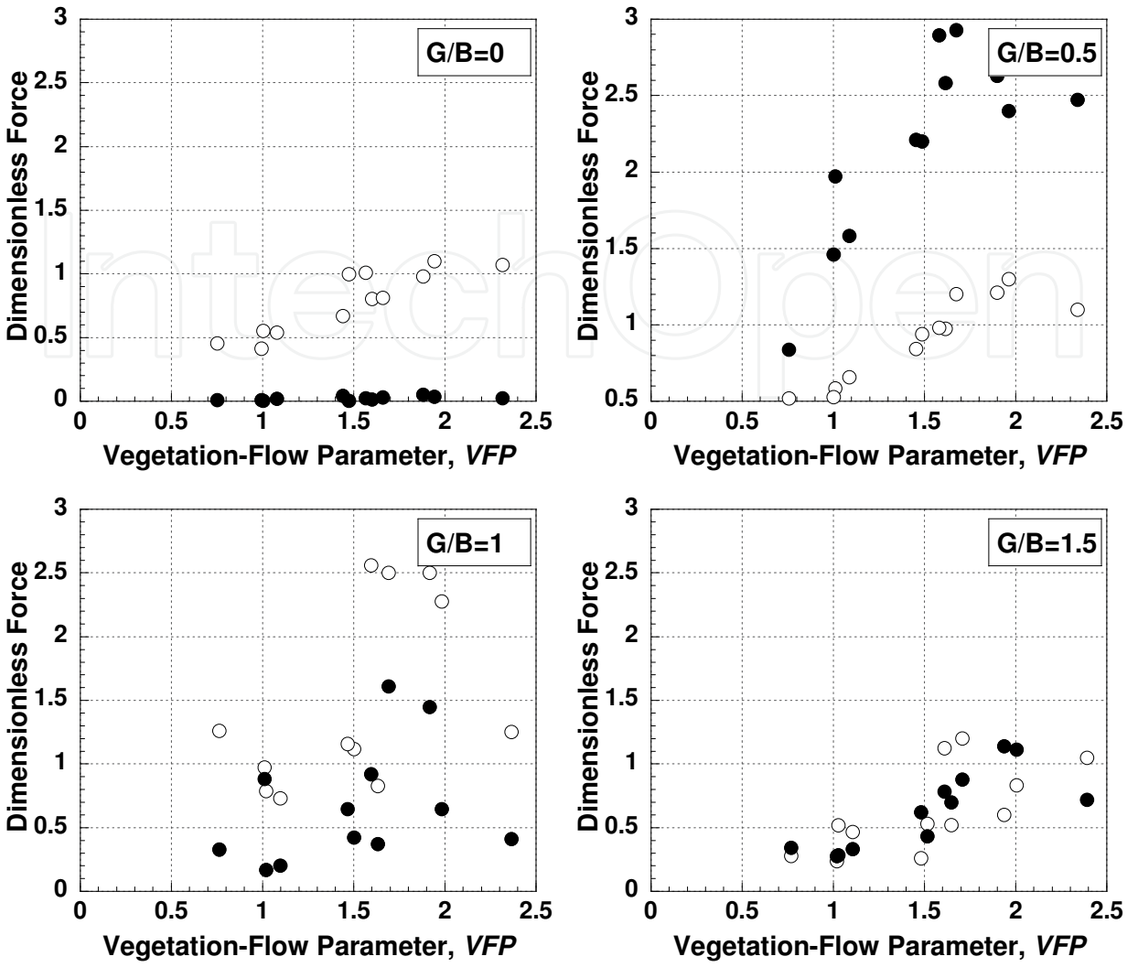

Fig.18. Variation of Dimensionless Force with Vegetation-Flow Parameter for (BG^*SP/D^2)=375 (○-No Veg and ●-Veg)

between rear face of vegetal patch and the front face of building); the maximum dimensionless force in the presence of vegetation is found to be about 80 - 95% less than that with vegetation. As *VFP* increases the force on the structure in the absence of vegetation is found to increase, whereas, this effect is not found to be significant when vegetation is present in front of the structure. For the case of *G/B*=0.5, the forces are clearly seen to increase for the structure fronted by vegetation, the rate of increase being higher with an increase in *VFP*. For the case of *G/B* = 1, although a similar trend in its variation as observed for *G/B*=0.5 is seen, the rate of increase in the force is found to much lesser. For the last case of *G/B* = 1.5, the forces in the presence of vegetation is found to be less compared to that obtained for the earlier two cases. It is observed that for the gap ratios <1.5, there is significant standing wave formation in the space between vegetation and building leading to the increase in the force. In addition, the kinetic energy of the reformed wave on the lee side of the vegetation may be more incase of *G/B* = 0.5 while this effect reduces as *G/B* increases. Hence most favorable location for the structure is adjacent to the green belt (*G/ B* =0) or away from the green belt by more than 1.5*B*. The maximum value of the dimensionless force is 1.2, 3, 2.6 and 1.3 for *G/B*=0, 0.5, 1, 1.5 respectively.

It is also observed that the F^* has a linear relationship with VFP for a given $[BG^*SP/D^2]$. Further, most of the points pertaining to G/B = 1.5 shows that the forces are mostly lower incase of buildings fronted by vegetation that the case of no vegetation. Hence it may be concluded that the value of G/B > 1.5 will yield beneficial effects incase of bio-shield. However the force reduction incase of G/B>1.5 could not be quantified as such a scenario was not included in the present experimental program. Considering the fact that all experiments are conducted for high Ursells parameter ($U_r \geq 180$), the above discussion indicates that G/B=0 and G/B>1-5 will be certainly beneficial against disastrous waves.

4. Summary and conclusions

A comprehensive experimental program was carried out for investigation of the interaction of emergent vegetation of different characteristics with uniform steady open channel flow as well as with waves of high Ursell's parameter. The study involved measurement of energy loss in the experiments in open channel. In addition, measurement of pressures on a vertical wall and forces on a model building, both placed at the shoreline and wave run up on the beach with a slope of 1:30, have been carried out in a wave flume.

An essential aspect of the present study is that the hydro elastic regime of the present problem, pertaining to plantations along open coasts, has been modelled using Froude law. The effects of canopy and leaf area, wind, surface roughness of the vegetal stems etc are not considered.

The resistance due to vegetation in a steady-uniform flow have been presented and discussed in terms of Darcy's-Weisbach friction factor f and Manning's friction co-efficient n in both Regular and Staggered configuration of elastic cylindrical stems emerging the water surface. The friction factors have been investigated in terms of Re, Fr, Reduced Velocity (V_r) and vegetation-flow parameter (VFP). The Vegetation-Flow Parameter is a newly proposed non-dimensional parameter to represent the relative elasticity of vegetal stems with respect to flow characteristics. Based on the above studies, new semi empirical relationships are proposed for f, n and E_L (energy loss) for all the flow regimes tested in terms of Fr and VFP.

It is concluded from the wave flume experiments that the Staggered configuration of the vegetation can serve as a better attenuator of waves, thus leading to lesser pressures on a vertical wall on its leeside for all the flow and vegetal parameters considered in the study. The pressures reduce on the wall by about 15-30% for regular vegetal configuration and by about 30-60% for Staggered vegetal configurations.

The non-dimensional run-up increases linearly as the surf similarity parameter increases. The percentage reduction of run-up due to waves in the presence of the vegetation is about 40% for the higher surf similarity parameter. R_u /H on the slope decreases in presence of Green Belt, the rate of reduction being significant to an extent of about 60% for Cnoidal waves for higher values of ξ, that is, long waves propagating over a slope. For larger width of green belt, the run-up is independent of the porosity, as shown using the SP/D parameter, of the vegetation. The percentage reduction of run-up is more for lesser BG of lesser porosity. The effect of vegetation is to reduce the R_u/H_s by about 40 %. This is valid for all the Vegetal parameter investigated.

The results on the variation of forces on a structure positioned at different distances from the green belt and subjected to the action of Cnoidal waves are presented and discussed in detail. The parameter, $[BG^*SP/D^2]$ is found to be quite useful in understanding the effects of placement of vegetation in combination with the width of green belt on the forces, F^*. On

the other hand *G/B*=0 or *G/B*>1.5 has been found to be suitable for the green belt to be effective in reducing theforces on the structure on its lee side, while *G/B*=0.5 has been found to cause adverse effect.

5. References

Carrier, G.F. and Greenspan, H.P. (1958). Water waves of finite amplitude on a sloping beach. *Journal of Fluid Mechanics*, 4, 97-109.

Carrier, G.F., Wu, T.T. and Yeh, H. (2003). Tsunami run-up and draw-down on a plane beach. *Journal of Fluid Mechanics*, 475 (1), 79-99.

Chen,C.I. (1976). Flow resistance in board shallow grassed channels. *Journal of the Hydraulics Division*, ASCE 102 (3), pp 307-322.

Chakrabarti, S.K. (1983). Hydrodynamics of offshore structures. Computational Mechanics Publications, Southampton Boston.

Darby, S. E. (1999). Modeling effect of riparian vegetation on flow resistance and flood potential. *J. Hydraul. Eng.,* 125. pp 443–454.

Dudley, F.S.J., Abt, S.R., Bonham, C.D., Watson, C.C., and Fischenich, J.C. (1998). Evaluation of flow-resistance equations for vegetated channels and floodplains. *Technical Report EL-98-2. U.S. Army Engineer Research and Development Center, Vicksburg, MS.*

Fathi-Moghadam, M. and Kouwen, N., (1997). Nonrigid, nonsubmerged, vegetative roughness on floodplains. *Journal of HydraulicEngineering* 123 (1), 51–57.

Fathi-Moghadam, M. (2006). Effects of land slope and flow depth on retarding flow in non-submerge vegetated lands. *J. Agron.ANSI*.5 (3), pp 536-540.

Fathi-Moghadam, M. (2007). Characteristics and mechanics of tall vegetation for resistance to flow, *African jr of biotechnology* Vol.6 (4), pp 475-480.

Fischenich, C. (2000). Resistance due to vegetation, *EMRRP Technical Notes*, *ERDC TN-EMRRP-SR-07, US Army Engineer Research and Development Center, Vicksburg, MS.*

Freeman, G. E. (1997). Analysis and prediction of plant stiffness modulus for selected plants. *Federal Contract No. DACW-39-97-M-1413, U.S. Waterway Experiment Station, U.S.Army Corps of Engineers*, Vicksburg, Miss.

Freeman, G.E., Rahmeyer, W. H. and Copeland, R. R. (2000). Determination of resistance due to shorts and woody vegetation. *Rep.ERDC/CHL TR-00-25, Engineer Research and Development Center,U.S. Army Corps of Engineers.*

Fuehrboeter, A. (1993). Wave loads on seadikes and seawalls. In: Abbott, M.B., Price, W.A. (Eds.), Coastal,Estuarial and Harbour Engineer's Reference Book. Chapman & Hall, London, pp. 351–367.

Furukawa, K., Wolanski, E., Mueller, H. (1997). Currents and sediment transport in mangrove forests. *Estuarine and Coastal Shelf Science* 44(3), 301-310.

Gan, K.S., Lim, S.C., Choo, K.T., Jantan, M.D. (2001). Timber notes-medium hardwoods 4. *Timber Technology Bulletin* 21, 1-7.

Goda, Y. (1974). New wave pressure formula for composite breakwater, *Proceedings of the 14th International Conference on Coastal Engineering, Copenhagen, Denmark* (1974) pp. 1702–1720.

Hall Jr, J.V. and Watts, G.M. (1953). Laboratory Investigation of the vertical rise of solitary waves on impermeable slopes Techincal Memorandum No.33, Beach Erosion Board, U.S.Army corps of Engineers, Washington, DC.

Hamzah, L., Harada, K., Imamura, F. (1999). Experimental and numerical study on the effect of mangrove to reduce tsunami. *Tohoku J. Nat. Disaster Sci.* 35(2), 127-132.

Harada, K. and Imamura, F. (2005). Effects of coastal forest on tsunami hazard mitigation – A preliminary investigation. Tsunamis, Case Studies and Recent Developments, Springer, Netherlands, pp. 279-292.

Hughes, S.A. (2004). Estimation of wave run-up on smooth, impermeable slopes using the wave momentum flux parameter, *Coastal Engineering*, Vol 51, pp- 1085-1104.

Jarvela,J. (2002). Determination of flow resistance of vegetated channel banks and flood plains. In River flow 2002,(Eds.Bousmar,D.and Zach,Y.) Lisse,Swets Zeitlinger, pp 311-318.

Järvelä, J. (2004). Determination of flow resistance caused by non-submerged woody vegetation, *Int. J. River Basin Manage.* 2 (2004) (1), pp. 61–70.

Kothyari, U.C, Hayashi, K., Hashimoto, H. (2009). Drag coefficient of unsubmerged rigid vegetation stems in open channel flows. *J. Hydraulic Res.* 47(6), 691-699.

Kouwen, N. and Li, R.M. (1980). Biomechanics of vegetative channellinings. *Journal of the Hydraulics Division*, ASCE 106 (6), 1085–1103.

Kouwen, N. and Fathi-Moghadam, M. (2000). Friction factors for coniferous trees along rivers. *Journal of Hydraulic Engineering*, ASCE, 126(10), pp 732-740.

Kutija, V., Hong, H.T.M., (1996). A numerical model for assessing the additional resistance to flow introduced by flexible vegetation. *J. Hydraulic Res*. 34(1), 99-114.

Li, Y. and Raichlen, F. (2001). Solitary wave run-up on plane slopes., *Journal of Waterway Port, Coastal and Ocean Engineering*, Vol. 127, pp. 33–44.

Liu, P., Lynett. and Wu, T. (2002). Modeling wave run-up with depth integrated equations, *Journal of Waterways, Port, Coastal and Ocean Engineering, ASCE* 46, pp. 89–107.

Meijer, D.G. and Van Velzen, E.H. (1999). Prototype-scale flume experiments on hydraulic roughness of submerged vegetation, *Proceedings of XXVIII AIHR Conference, Graz (A), Sept. 1999.*

Mueller and Whittaker, (1993). G.U. Muller and T.J.T. Whittaker, An investigation of breaking wave pressures on inclined walls, *Ocean Engineering* 20 (4) (1993), pp. 349–358.

Nepf, H.M. (1999). Drag, turbulence and diffusion in flow through emergent vegetation. *Water Resources. Res,*. 35 (2), pp 479–489.

Noarayanan, L., Murali, K. and Sundar, V. "Wave attenuation by flexible vegetation on a mild slope"Proc. International Conference in Ocean Engineering-2-5 Feb 2009 IIT Madras, INDIA, pp 1157-1169

Petry.K.S. and Bosmajian,G.B. (1975). Analysis of flow through vegetation. *Journal of hydraulic division*.ASCE 101(7), pp 871-884.

Ree, W.O. and Crow, F.R. (1977). Friction factors for vegetated waterways of small slope. *Agricultural Research Service* ARS-S-151. U.S. *Department of Agriculture, Washington, D.C.*

Righetti, M., and Armanini, A. (2002) Flow resistance in open channel flows with sparsely distributed bushes." *J. Hydrol.*, 269_1–2_, 55–64.

Sarpkaya, T. and Isaacson, M. (1979) Mechanics of wave forces on offshore structures, Van Nostrand reinhold company , New york, pp-420(to be removed)

Synolakis, C.E. (1986). The run-up of solitary waves. Journal of Fluid Mechanics vol. 185. Cambridge University Press, United Kingdom, pp. 523-545.

Tanaka, N. (2009). Vegetation bio-shields for tsunami mitigation: Review of effectiveness, limitations, construction, and sustainable management. *J. Landscape and Ecological Eng*. 5(1), 71-79.

Timoshenko, S.P. and Gere, J.M. (1961). *Theory of elastic stability, McGraw Hill, New York.*

Werth, D. (1997). Predicting flow resistance due to vegetation in flood-plains, *PhD thesis, Utah State University, Logan, Utah.*

Yang, W. and Choi,S.U (2009). Impact of stem flexibility on mean flow and turbulence structure in open-channel flows with submerged vegetation. Jl. Hydraulic Res. 47 (4), 445-454.

Zdravkovich, M.M. and Medeiros, E.B. (1991). Journal of Wind Engineering and Industrial Aerodynamics. *Elsevier Science Publishers* B.V.,Amsterdam – Printed in The Netherlands, 38 pp 197-211.

The Tsunami Threat - Research and Technology

Edited by Nils-Axel MÃ¶rner

ISBN 978-953-307-552-5
Hard cover, 714 pages
Publisher InTech
Published online 29, January, 2011
Published in print edition January, 2011

Submarine earthquakes, submarine slides and impacts may set large water volumes in motion characterized by very long wavelengths and a very high speed of lateral displacement, when reaching shallower water the wave breaks in over land - often with disastrous effects. This natural phenomenon is known as a tsunami event. By December 26, 2004, an event in the Indian Ocean, this word suddenly became known to the public. The effects were indeed disastrous and 227,898 people were killed. Tsunami events are a natural part of the Earth's geophysical system. There have been numerous events in the past and they will continue to be a threat to humanity; even more so today, when the coastal zone is occupied by so much more human activity and many more people. Therefore, tsunamis pose a very serious threat to humanity. The only way for us to face this threat is by increased knowledge so that we can meet future events by efficient warning systems and aid organizations. This book offers extensive and new information on tsunamis; their origin, history, effects, monitoring, hazards assessment and proposed handling with respect to precaution. Only through knowledge do we know how to behave in a wise manner. This book should be a well of tsunami knowledge for a long time, we hope.

InTech Europe
University Campus STeP Ri
Slavka Krautzeka 83/A
51000 Rijeka, Croatia
Phone: +385 (51) 770 447
Fax: +385 (51) 686 166
www.intechopen.com

InTech China
Unit 405, Office Block, Hotel Equatorial Shanghai
No.65, Yan An Road (West), Shanghai, 200040, China
中国上海市延安西路65号上海国际贵都大饭店办公楼405单元
Phone: +86-21-62489820
Fax: +86-21-62489821

IntechOpen